Defence Research and Development Canada
Recherche et développement pour la défense Canada

DEFENCE R&D DÉFENSE

A Review of Equation of State Models, Chemical Equilibrium Calculations and CERV Code Requirements for SHS Detonation Modelling

P. Thibault
TimeScales Scientific Ltd

Contract Scientific Authority: J. Lee, DRDC Suffield

Defence R&D Canada

Contract Report

DRDC Suffield CR 2010-013

October 2009

Canada

A Review of Equation of State Models, Chemical Equilibrium Calculations and CERV Code Requirements for SHS Detonation Modelling

P. Thibault
TimeScales Scientific Ltd
554 Aberdeen Street SE
Medicine Hat AB T1A 0R7

Contract Number: Subcontract under W7702-08R183/001/EDM

Contract Scientific Authority: J. Lee (403-544-5025)

Defence R&D Canada – Suffield

Contract Report

DRDC Suffield CR 2010-013

October 2009

A Review of Equation of State Models, Chemical Equilibrium Calculations and CERV Code Requirements for SHS Detonation Modelling

Paul Thibault

8 October 2009

Work performed for DRDC Suffield under contract to UTIAS

TimeScales Scientific Ltd.

Table of Contents

1. Introduction

This report discusses physical models, calculations and code capabilities for SHS detonation modelling. The main objectives of this study are to:

- Summarize currently available physical models and data,
- Perform calculations with various equilibrium codes for selected systems,
- Outline CERV code capabilities and limitations,
- Discuss the sections of the CERV code that would be impacted by the inclusion of new models,
- Assign priorities for model development and SHS system modelling.

2. Current Capabilities

2.1 Points and Processes

CERV [1] is currently capable of calculating the following thermodynamic points and processes:

- ***Thermodynamic Points***
  - Temperature-Pressure (TP)
  - Temperature-Volume (TV)
  - Pressure-Volume (PV)

- ***Processes***
  - Constant pressure combustion
  - Constant volume combustion
  - Detonation
  - Isentrope

A driver program has been written to perform various P-V plane calculations. The results of these calculations are then graphically displayed through a post-processing program. The plots generated include colour contours of various thermodynamic quantities and species concentrations as a function of pressure and volume They also include a display of the Rayleigh line and Hugoniot curve with constant pressure, constant volume and detonation combustion points.

2.2 Physical Models

CERV currently minimizes the Gibbs energy based on:

- NASA polynomials for the thermodynamic properties,
- Virial equation of state (EOS) for gases,
- Incompressible solids and liquids.

2.3 Current Limitations

The main CERV code limitations include:

- Gases
    - Although the third-order virial EOS, used in CERV, is suited to rocket applications where the pressures are of the order of 0.01 GPa, it may not be accurate for condensed explosives and SHS systems, where the detonation pressures are of the order of 5-50 GPa.
    - CERV does not currently include corrections for non-ideal mixtures.
- Condensed Species
    - CERV does not include an EOS that accounts for volume change due to compression or thermal expansion.
    - Specific volumes of condensed species do not differ between the liquid and solid phases and are often set to a default value of 2 g/cc.
    - The effect of pressure on the melting temperature is not considered.
    - No solution rule (ideal or non-ideal) is included. Consequently, separate melting temperatures are assigned to co-existing condensed species. Phase diagram topologies (eg. eutectic point) are therefore not modelled.

3. Available Modelling Approaches for Gases

3.1 Equations of State

A variety of equations of state have been proposed to model non-ideal gases. These include classic text book models [2-4] such as :

- van der Waals
- Redlich-Kwong
- Beattie-Bridgeman
- Virial expansion

The above equations are suitable for moderate pressures and are usually based on either empirical constants, molecular parameters and potentials, or on the law of corresponding states. Potentials typically used for virial expansion coefficient calculations include the hard sphere, square well, Lennard-Jones (6-12) and n-6-8 potentials [3].

The detonation of a condensed explosive generates very high pressures of the order of 20 GPa. For such pressures, the most popular equations of state include those discussed by Davis [5]. These include:

1. Becker-Kistiakowsky-Wilson (BKW)
2. Jacobs-Cowperthwaite-Zwisler (JCZ)
3. Hayes
4. Davis
5. Williamsburg
6. JWL
7. HOM

the JWL and HOM EOS have often been used in hydrocode/CFD simulations. On the other hand, the BKW and JCZ equations remain the EOS of choice in chemical equilibrium code development for condensed explosives.

Various databases have been constructed for the BKW and JCZ equations of state. These include:

- BKWC, BKWR and BKWS (Sandia)
- JCZ2, JCZ3 and JCZS (Sandia)

BKW coefficients are empirical and usually based by fitting detonation performance data. The JCZ coefficients are more physics-based and have traditionally been obtained from intermolecular potentials. Due to the limited available data for potential parameters, some JCZS coefficients have also been obtained through the method of corresponding states and matching with BKW coefficients. An excellent description of the various approaches can be found in the Sandia report by McGee, Hobbs and Baer [6], who provide a database of JCZS parameters for a large number of species. These authors provide many sample calculations with the JCZS database incorporated in CHEETAH 2.0, including comparisons with experimental data for gases and liquids. Sample comparisons are shown in Figures 1 and 2.

3.2 Mixture Rules

Mixtures of gaseous species are assumed 'ideal' when the total volume of the mixture may be approximated as the sum of the partial volumes from each specie. A more realistic 'non-ideal' mixture model takes into account the fact that the equation of state coefficients for one specie depends on the concentrations of other species in the mixture. Various approaches to modelling non-ideal mixtures are discussed in the book by Poling, Prausnitz and O'Connel [7], which describes methods based on either intermolecular potentials or on the method of corresponding states.

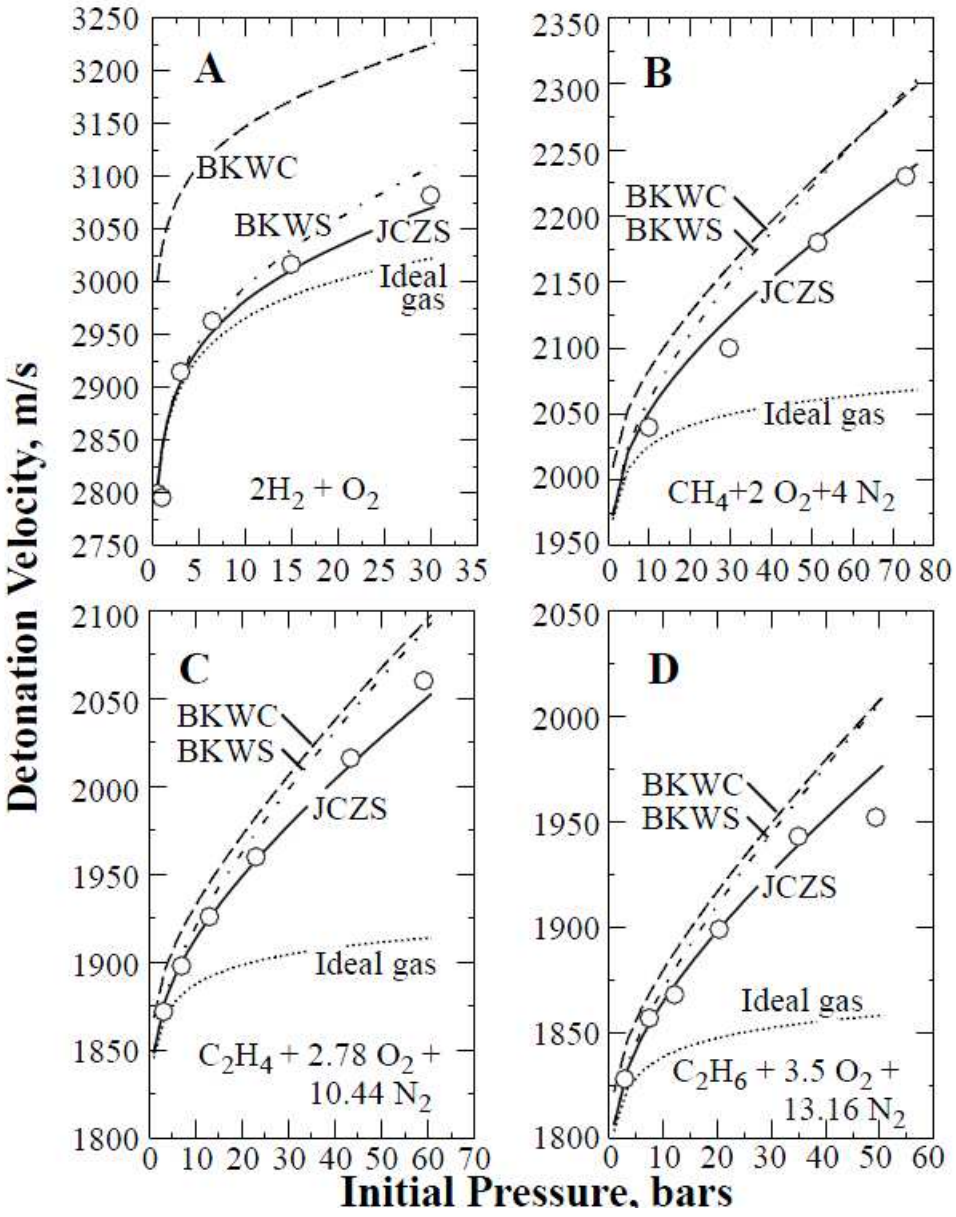

Figure 1: Comparisons of experimental (circles) and computed (lines) data for gaseous detonation velocities using different equations of state (from McGee et al [6])

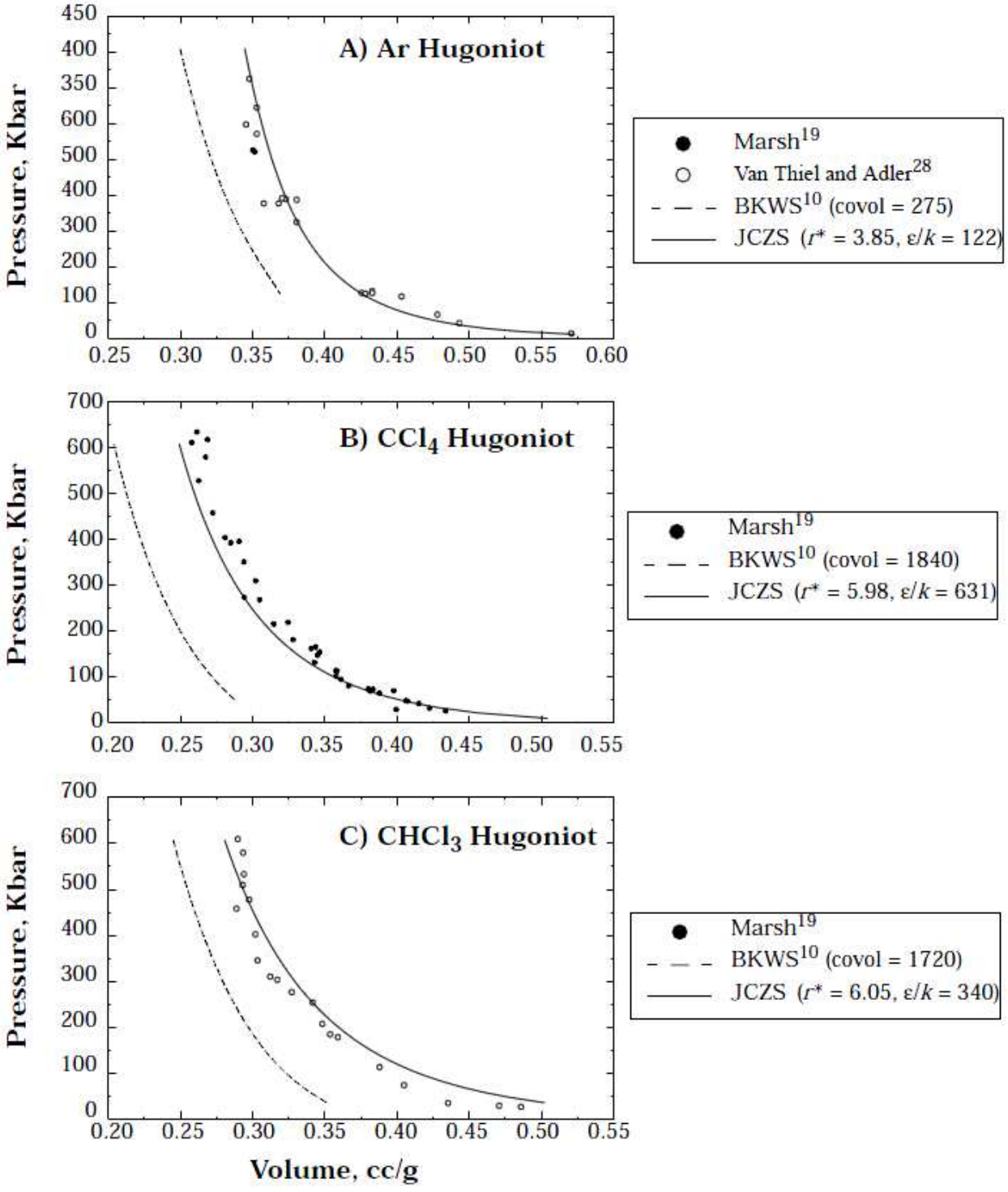

Figure 2: Comparisons of experimental (circles) and computed (lines) data for liquid shock pressures using different equations of state (from McGee et al [6])

4. Available Modelling Approaches for Condensed Species

4.1 Equations of State

A wide variety of equations of state have been proposed for condensed solid and liquid substances. It should be noted that various types of groups have been involved in developing equations of state and in determining model constants based on experimental measurements and ab initio calculations. The earth sciences community have been particularly active in this research area, with excellent summaries provided in the books by Poirier [8] and Anderson [9]. Other areas of applications include detonics, material sciences and underwater explosions. Recent reviews in the field of detonics may be found in the book chapters by Peiris et al [10] and Dattelbaum et al. [11]. The most common methods to determine the EOS parameters include:

- Diamond Anvil Cell (DAC) in conjunction with X-Ray diffraction measurements,
- Shock Hugoniot measurements,
- Detailed theoretical ab initio calculations.

Generally speaking, the EOS should address the static 'cold' compression properties, where the temperature is maintained at a reference state, as well as the 'thermal effect' when the material is heated to temperatures above this state. The thermal effect is closely related to the thermal expansion properties of the substance. The total pressure, p, of a substance is therefore often written as:

$$p = p_c + p_{th}$$

where p_c is the 'cold' contribution and p_{th} is the thermal contribution.

4.2 Cold Compression

The most commonly used cold compression EOS include:

- Simple bulk modulus relation
- Birch-Murnaghan (second- and third-order) equations
- Logarithmic equation
- Vinet equation

The brief summary below is partly based on the more detailed discussion in Poirier`s book.

4.2.1 Simple Bulk Modulus Equation

The simplest compressibility model is based on linear elasticity where the strain is proportional to the stress. For volumetric compression, the change in pressure may be expressed in terms of the change in volume through the relationship:

$$\frac{dv}{v} = -\frac{dp}{K}$$

which may also be written as:

$$K = -\frac{dp}{d\ln v}$$

where K is the bulk modulus. For an isotropic solid, K may be expressed in terms of the Young's modulus Y, and the Poisson ratio, μ, as:

$$K = \frac{Y}{[3(1-2\mu)]}$$

It should be noted that different definitions exist for the bulk modulus depending on the thermodynamic variable that is held constant in the derivative of pressure. The bulk moduli K_T and K_s usually denote constant temperature and constant entropy bulk moduli respectively. The two are related through the equation:

$$K_T = K_s/\left[1 + TV\alpha^2 K_s/C_p\right]$$

where α and Cp are the thermal expansion and constant pressure heat capacity respectively [12].

4.2.2 Murnaghan, Tait and Sun EOS

The Murnaghan equation of state is based on the laws of elasticity and the assumption that the bulk modulus is proportional to pressure. The pressure may then be expressed as:

$$p = \frac{K_o}{K'_o}\left[\left(\frac{\rho}{\rho_o}\right)^{K'o} - 1\right]$$

where the exponent, K'_o , is the initial derivative of the bulk modulus with respect to pressure and has a typical value of 3.5 for solid metals. The above equation is similar to one of the many forms of the Tait equation of state, which is commonly used for liquids. As indicated by Dattelbaum et al. [11] in reference to explosive binders, materials displaying many phases may be described by the more general Sun equation of state:

$$p = \frac{K_o}{(n-m)}\left[\left(\frac{\rho}{\rho_o}\right)^{n+1} - \left(\frac{\rho}{\rho_o}\right)^{m+1}\right]$$

which is similar in form to the Birch-Murnaghan EOS discussed below.

4.2.3 Birch-Murnaghan and Logarithmic EOS

The Birch-Murnaghan is based on the finite Eulerian strain and a power expansion of the Helmholtz energy in terms of a parameter related to the density ratio. The second-order and third-order expansions result in the following equations:

$$p = \frac{3K_{oT}}{2}\left[\left(\frac{\rho}{\rho_o}\right)^{7/3} - \left(\frac{\rho}{\rho_o}\right)^{5/3}\right]$$

$$p = \frac{3K_{oT}}{2}\left[\left(\frac{\rho}{\rho_o}\right)^{7/3} - \left(\frac{\rho}{\rho_o}\right)^{5/3}\right]\left\{1 + \frac{3}{4}(K'_o - 4)\left[\left(\frac{\rho}{\rho_o}\right)^{2/3} - 1\right]\right\}$$

with the third-order equation reducing to the second-order equation when $K'_o = 4$. The second-order equation can also be obtained through the selection of appropriate parameters in the interatomic Mie potential. The Birch-Murnaghan equation may also be formulated using a Lagrangian strain formulation. In a similar fashion, the following logarithmic equation is obtained through an expansion involving the Henky strain:

$$p = K_o \frac{\rho}{\rho_o} \ln \frac{\rho}{\rho_o}\left[1 + \left(\frac{K`_o - 2}{2}\right) \ln \frac{\rho}{\rho_o}\right]$$

4.2.4 Vinet EOS

Due to the power series expansions involved, the above equations lose their accuracy for very high pressures. The following Vinet equation addresses this issue by expressing the bulk modulus and its derivatives in terms of the interatomic distance and a scaling parameter. The following equation is then obtained for the volume ratio.

$$p = 3K_o \left(\frac{V}{V_o}\right)^{-2/3}\left[1 - \left(\frac{V}{V_o}\right)^{1/3}\right] e^{\left\{\frac{3}{2}(K'_o - 1)\left[1 - \left(\frac{V}{V_o}\right)^{1/3}\right]\right\}}$$

Poirier presents a useful plot comparing the different equations of state for different values of K_o' (Fig. 3). Although the results from different EOS are very similar for $K_o' = 3.5$, significant differences are observed for other values.

4.3 Thermal Pressure and Expansion

The thermal contribution, p_{th}, to the total pressure, p, can be described through the Mie-Gruneisen equation:

$$p_{th} = \gamma_{th} E_{th} / V$$

where E_{th} is the thermal energy and γ_{th} is the thermal Gruneisen coefficient. The thermal pressure is related to the thermal expansion which is the result of the intermolecular vibrations and the asymmetric intermolecular potential consisting of a short-range repulsive potential and a longer-range attractive potential. Under the quasi-harmonic assumption that the frequency modes are independent of temperature, the thermal Gruneisen coefficient is equal to the Debye Gruneisen coefficient, γ_D:

$$\gamma_{th} = \gamma_D = \frac{\alpha V K_T}{C_V}$$

where, α is the thermal expansion coefficient and C_V is the constant volume heat capacity.

Based on experimental data, Anderson [13], noted that the thermal pressure increases linearly with temperature unless the temperature is significantly below the Debye temperature, θ_D (Fig. 4).

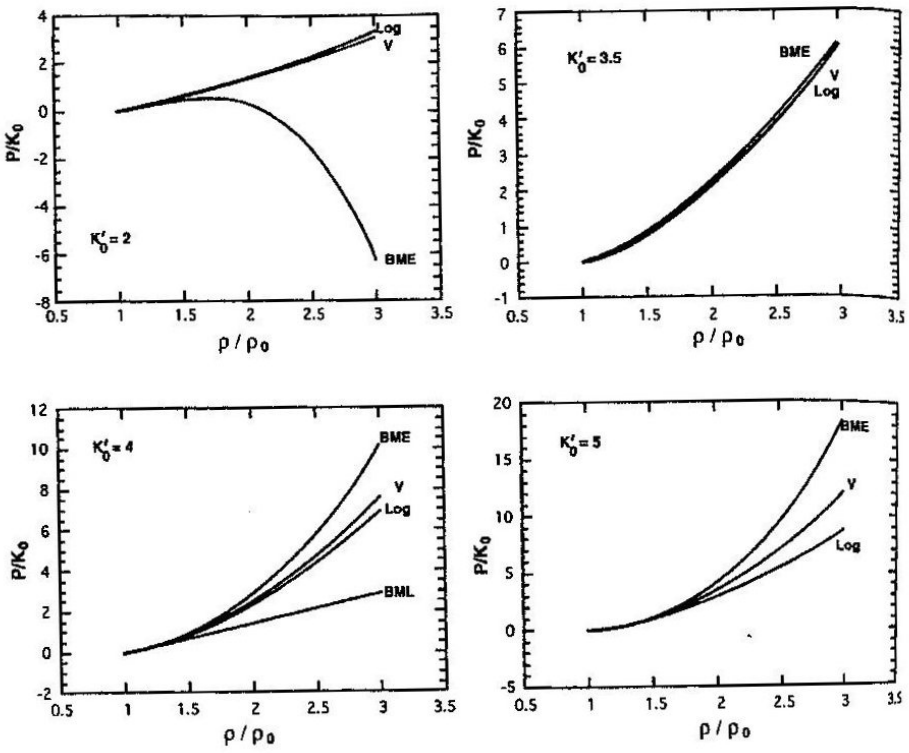

Figure 3: Comparison of results for normalized pressure vs. density ratio for different K'_o using different equations of state: BME: Birch-Murnaghan (Eulerian), BML: Birch-Murnaghan (Lagrangian), Log: Logarithmic, V: Vinet. (from Poirier [8])

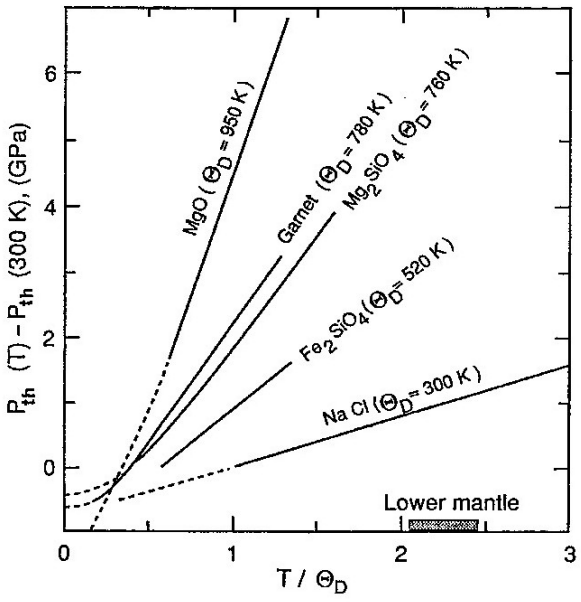

Figure 4: Dependence of thermal pressure on normalized temperature (from Poirier [8])

As a consequence of the above linear dependence, the thermal pressure may be written as [8]:

$$p_{th} = \int_0^T \left(\frac{\partial p}{\partial T}\right)_V dT = \int_0^T \alpha K_T dT = -\int_0^{\theta_D} \alpha K_T dt + \alpha K_T (T - \theta_D)$$

where αK_T is approximately constant for $T > \theta_D$. As shown in Figure 5 for MgO, the thermal expansion increases with temperature but decreases with pressure (Brosh et al. [14], Dubrovinsky and Saxena [15]). Chang [16] has developed a scaling law, based on the Debye temperature, that captures the temperature dependence of the thermal expansion coefficient for various metals (Figure 6).

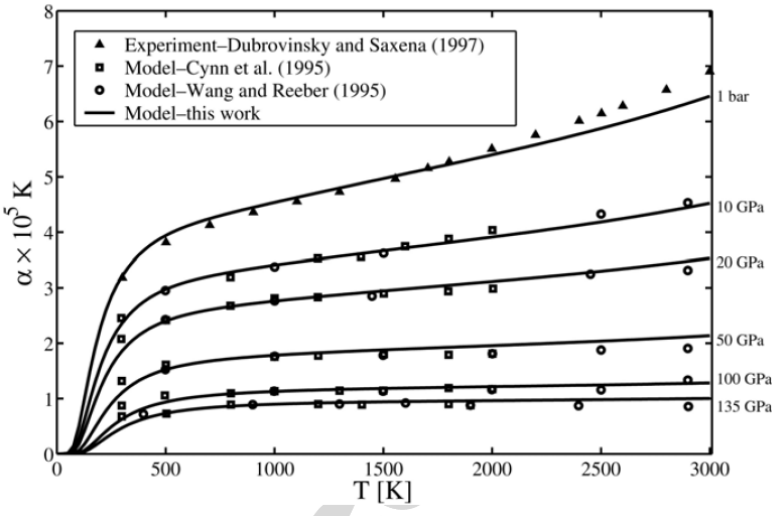

Figure 5: Dependence of thermal expansion coefficient on pressure and temperature for MgO (from Brosh et al. [14], experimental data from Dubrovinski et al. [15])

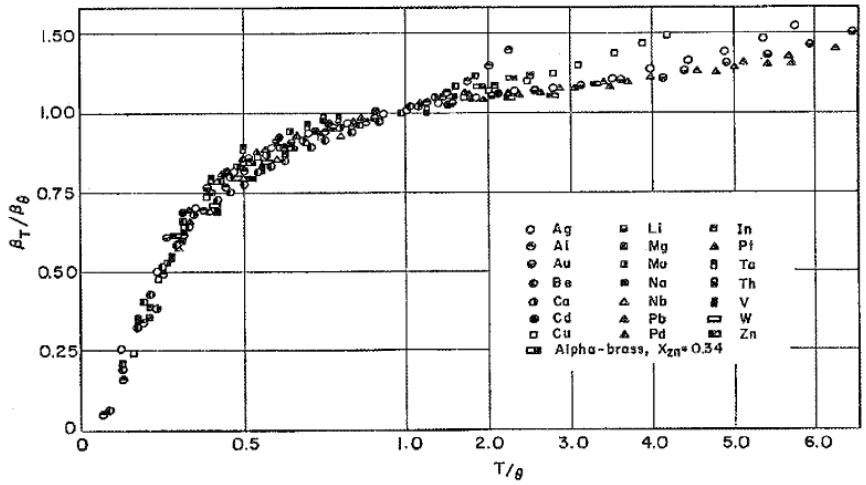

Figure 6: Normalized thermal expansion coefficient as a function of the normalized temperature for various metals (from Chang [16])

As previously mentioned, different reference states may be used in the Mie-Gruneisen equation. When cold isothermal compression data is available, the reference state corresponds to the temperature at which the experiments are performed. On the other hand, if Hugoniot data are used, the reference state corresponds to a point on the Hugoniot curve. Gheribi et al. [17] have derived an interesting methodology relating the Hugoniot and cold compression curves for metals. They observed that the two curves have similar shapes and can be related by assigning a larger stiffness (or effective interatomic potential) to the material for the shock Hugoniot. Their results indicate that the ratio of the "effective" bulk modulus for the Hugoniot over the actual bulk modulus remains relatively constant. A similar observation is made for the first and second derivatives of these properties. So far, the methodology has only been applied to monatomic closely-packed metals.

Another method of including the thermal contribution in an equation of state is to allow the bulk modulus, K, and the first derivative n = K' = dK/dp to vary with temperature. Fernandez [18] has applied this method to the Murnaghan equation of state. The temperature dependence is calculated based on a Gruneisen coefficient for a Debye solid. The temperature dependence of n can be expressed as a second-order polynomial.

Many of the thermal pressure models described above are based on a Gruneisen coefficient which varies with volume. If the thermal Gruneisen coefficient, γ_{th} , is used, the variation of this coefficient can be quite reasonably approximated by assuming that the ratio $\frac{\gamma_{th}}{V}$ is constant. It should be noted that a variety of Gruneisen coefficients are used in the modelling of material properties. Some of these are based on material properties at the atomic level, while others are based on more macroscopic properties and measurements. A good description of the various Gruneisen coefficients is presented in Poirier's book. As noted by Vocadlo et al. [19], there exist significant differences between the various Gruneisen coefficients and those calculated from detailed ab initio calculations. A judicious choice of a suitable Gruneisen coefficient must be made when applying it to a particular equation of state or Hugoniot. This point has also been emphasized by Segletes [20].

4.4 Melting of Metals

4.4.1 Melting Parameters

Melting of a material is associated with the loss of resistance to shear and long-range crystalline order. Some important parameters associated with melting include:

- The melting temperature T_m, which depends on the pressure,
- The change in volume $\Delta V_m = V_L - V_S$ between the liquid and solid state,
- The change in entropy $\Delta S_m = S_L - S_S$ between the liquid and solid state,
- The latent heat of melting $L_m = T_m \Delta S_m$.

4.4.2 Clausius-Clapeyron Equation

The simplest equation relating the above parameters is that of Clausius-Clapeyron:

$$\frac{dT_m}{dp} = \frac{\Delta V_m}{\Delta S_m}$$

Knowing the melting temperature, the volume change and the latent heat of melting, the above equation may be used to obtain the initial linear dependence of the melting temperature with pressure near atmospheric pressure.

4.4.3 Equations Based on Lindemann Law

As seen from Figure 7 [21], the linear Clausius-Clapeyron relationship is no longer valid for higher pressures, with the non-linearity being more pronounced for softer materials. The most popular models to predict this nonlinear dependence are based on the law of Lindemann [22]. Poirier presents an excellent description of this law with the extension developed by Gilvarry [23]. Further modifications to these models have also been presented by Schossler et al. [21] and Fang et al. [24].

The original Lindemann-Gilvarry model is based on the notion that the melting point is based on a critical level of atomic vibrations relative to the interatomic distance r_m. Following the discussion by Poirier [8], the melting criteria is then presented as:

$$\langle u^2 \rangle = f^2 r_m^2$$

where $\langle u^2 \rangle$ is the mean-square atomic velocity and f is an empirical constant that is approximately 0.08 for metals. For high temperatures and a monoatomic solid, $\langle u^2 \rangle$ may be estimated as:

$$\langle u^2 \rangle = \frac{9h^2 T}{m k_B \theta_D^2}$$

where, m is the atomic mass, θ_D is the Debye temperature and h and k_B are the Planck and Boltzmann constants respectively. The melting temperature is then given as:

$$T_m = f^2 \frac{k_B}{9h^2} m \theta_D^2 r_m^2$$

Lennard-Jones and Devonshire [25] have provided a theoretical justification of the empirical Lindemann-Gilvarry model based on the Lennard-Jones potential. Since r_m varies with pressure and is related to the specific volume, the Lindemann law is usually used in conjunction with an equation of state to determine the pressure dependence of the melting temperature.

As can be seen from the calculations of Schossler et al. [21] (Figure 7) and Fang et al [24], predictions based on the Lindemann-Gilvarry approach provide good agreement for monoatomic metals. As indicated by Poirier, however, the predictive capability of the models are significantly lower for more complex molecules. As will be discussed below, some of these limitations have been addressed in the more recent work of Shen et al. [26-27] and Wang et al. [28-29] and by more detailed and fundamental ab initio calculations.

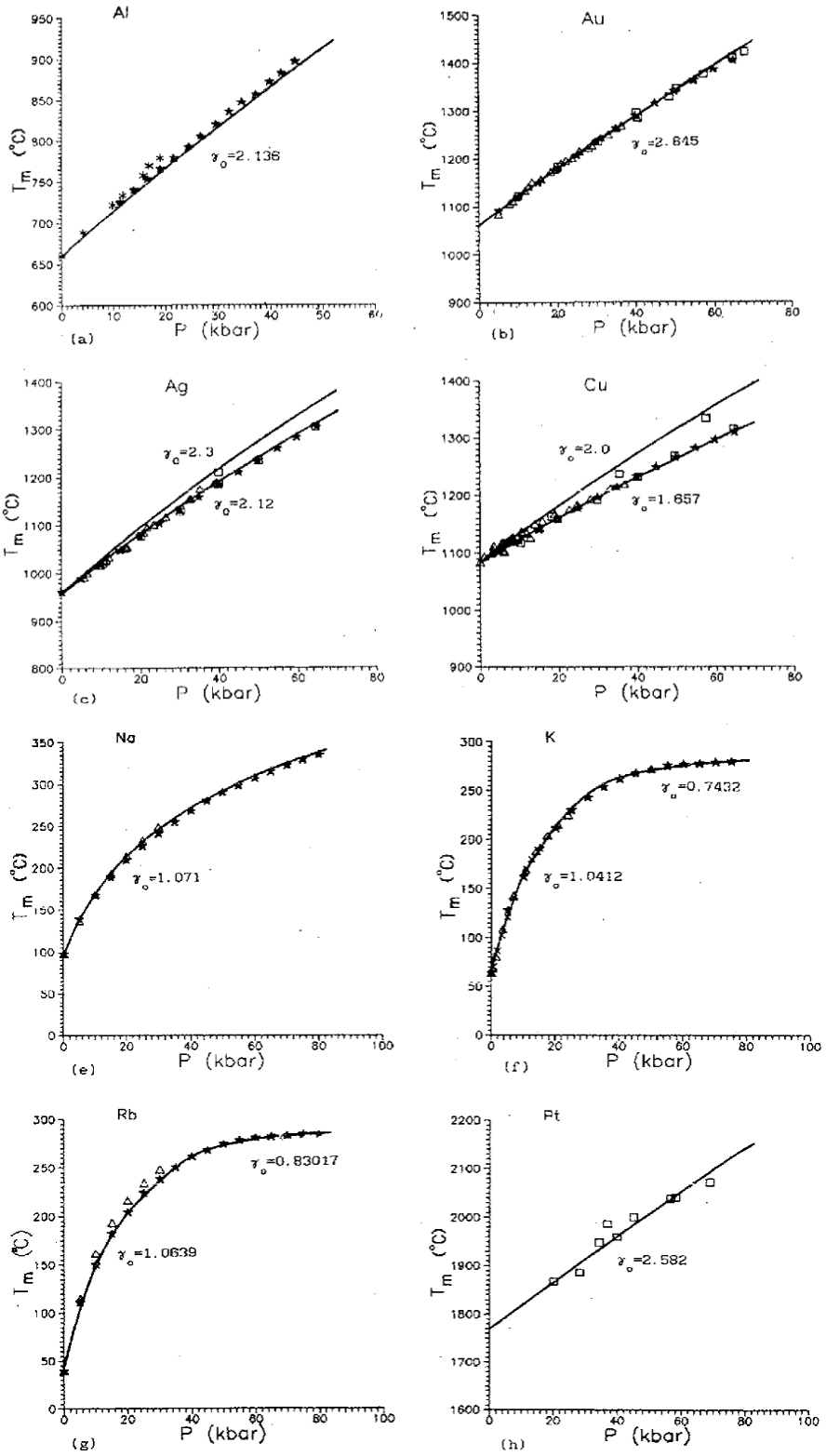

Figure 7: Dependence of melting temperature on pressure. Solid lines represent model predictions, (from Schlosser et al. [21]).

4.4.4 Models based on Volume Change

Useful relationships have been derived between the entropy and volume changes ΔS_m and ΔV_m for melting. Oriani [31] and Tallon [32] proposed the relationship:

$$\Delta S_m = Rln2 + \alpha K_T \Delta V_m$$

The first and second terms are the configurational and thermal entropy respectively. Since αK_T is approximately constant, the above relationship implies that the entropy change is proportional to the volume change. The entropy change can be expressed in terms of the melting temperature and the latent heat of melting. The entropy change associated with melting has been estimated by Wallace [32] for 25 elements.

4.4.5 Wang, Lazor and Saxena Model

As previously indicated, the Lindemann-Gilvarry model has been applied most successfully to monoatomic metals for pressures below 10GPa. Wang et al. [29] have developed a simple thermodynamic model that has been applied to polyatomic molecules for pressures as high as 100 GPa. The model is based on calculating the 'critical' melting temperature, which is related to a critical volume. The procedure relates the pressure-dependent melting temperature to thermodynamic properties at ambient pressure. These include the isothermal bulk modulus and the solid molar volume at room temperature, the isothermal bulk modulus and liquid molar volume at the melting point, the bulk modulus derivative, and the average product of the thermal expansion and the bulk modulus. The analysis is based on the Birch Murnaghan EOS and a thermal pressure which, as previously discussed, is related to the product of the thermal expansion coefficient, the isothermal bulk modulus and temperature differential. Computations and comparisons with experiments have been performed for lithium fluoride (LiF), diopside ($CaMgSi_2O_6$) and wustite (FeO). As seen from Figure 8 for LiF, the model calculations compare very well with experimental data for pressures as high 95 GPa. The model is also significantly more accurate than the Lindemann model at higher pressures. It can also be seen from Figure 9 that the model provides data for the thermal pressure and the melting molar volume as a function of pressure. This type of data is of particular relevance to assessing the SHS detonation potential of a system.

4.5 Experimental Data and Ab Initio Calculations

The data required for the various EOS parameters and melting properties models may be obtained from experimental data or ab initio calculations based on fundamental intermolecular potentials and quantum statistical mechanics. High pressure experimental data are usually obtained from Diamond Anvil Cell (DAC) or shock Hugoniot measurements. Ab initio calculations are based on molecular dynamics calculations using the Density Functional Theory (DFT). A description of the DFT methodology can be found in computational chemistry text books such as that by Cramer [34]. Figure 10, from Cazorla et al. [35], displays comparisons between experimental and theoretical data for the shock Hugoniot and melting temperature of molybdenum. Figures 11 and 12, from Alfe et al. [36,37], display similar comparisons for Al and MgO. An overview of ab initio modelling capabilities for the calculation of melting properties can be found in the article by Alfe et al. [36].

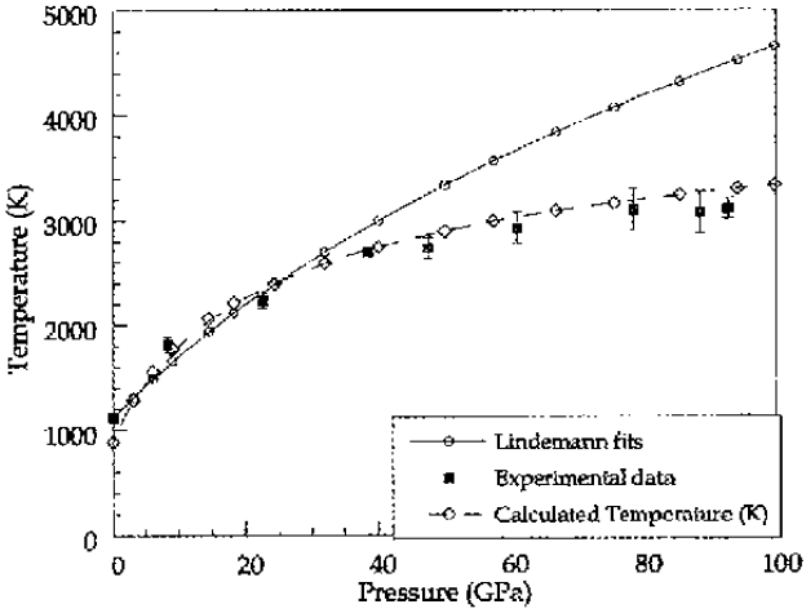

Figure 8: Melting temperature predictions using Wang et al. and Lindemann models, and experimental data for LiF system [29].

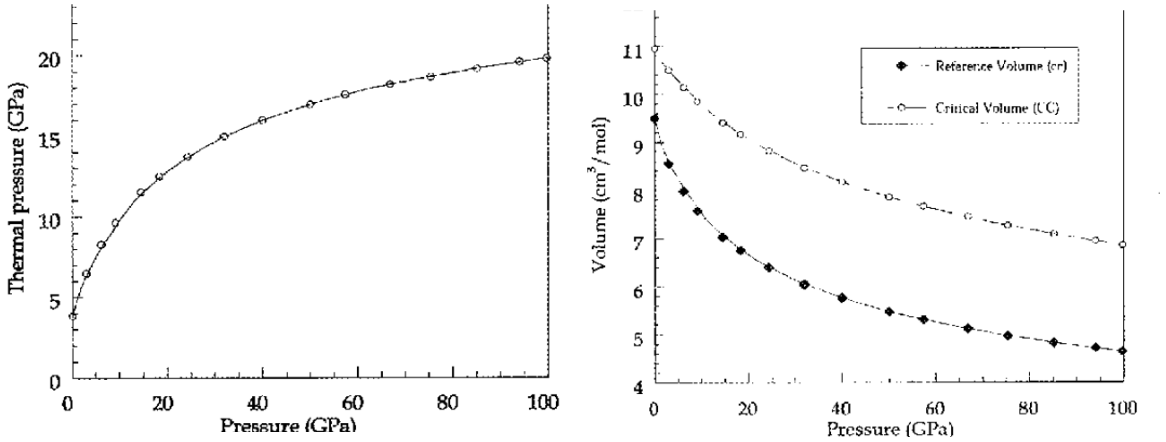

Figure 9: Melting thermal pressure and molar volume predictions using Wang et al. model for LiF system [29].

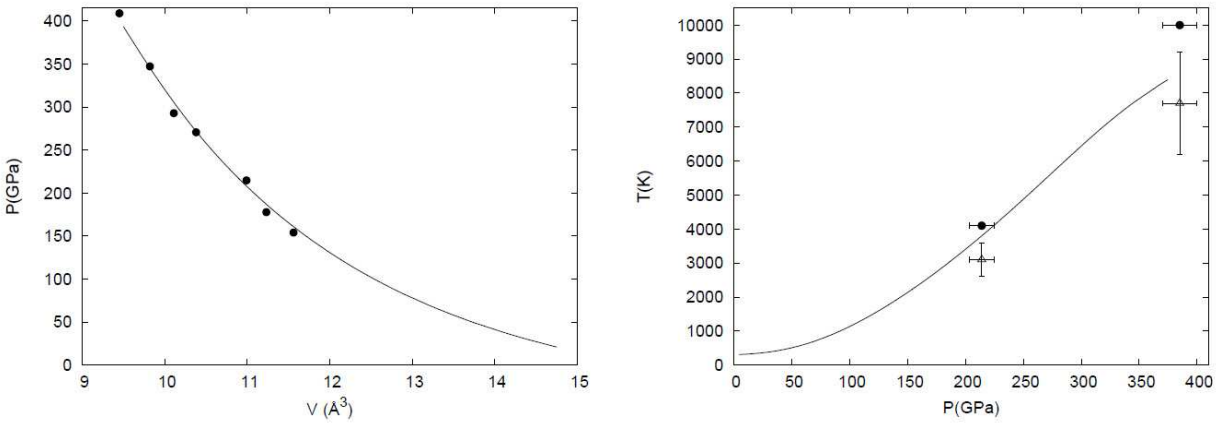

Figure 10: Comparisons of experimental and ab initio data for the Hugoniot and melting temperature of molybdenum, from Carzola et al. [35]

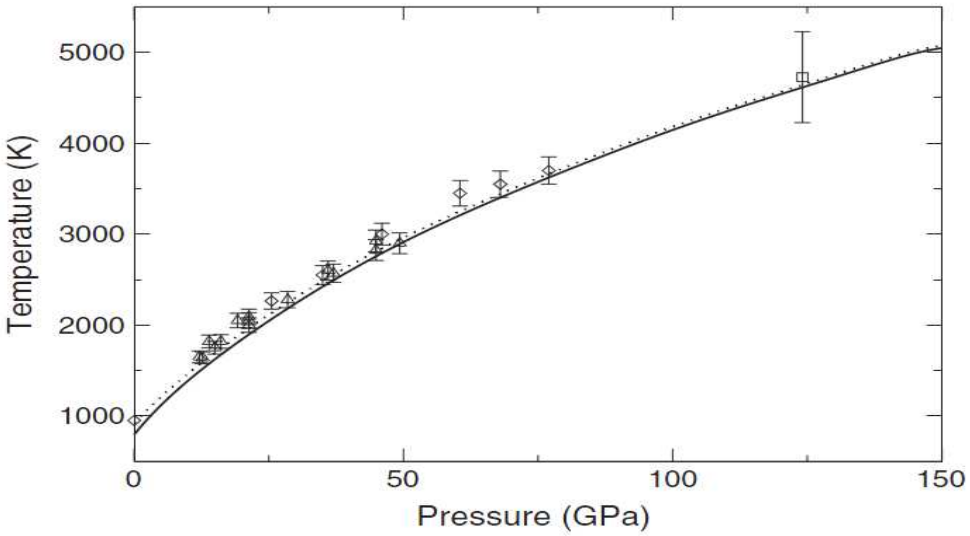

Figure 11: Comparisons of experimental and ab initio data for the melting temperature of Aluminium, from Alphe et al. [36]. Solid and dotted lines are ab initio results. Diamonds and square denote the experimental DAC and Hugoniot data.

4.6 Solution Rules

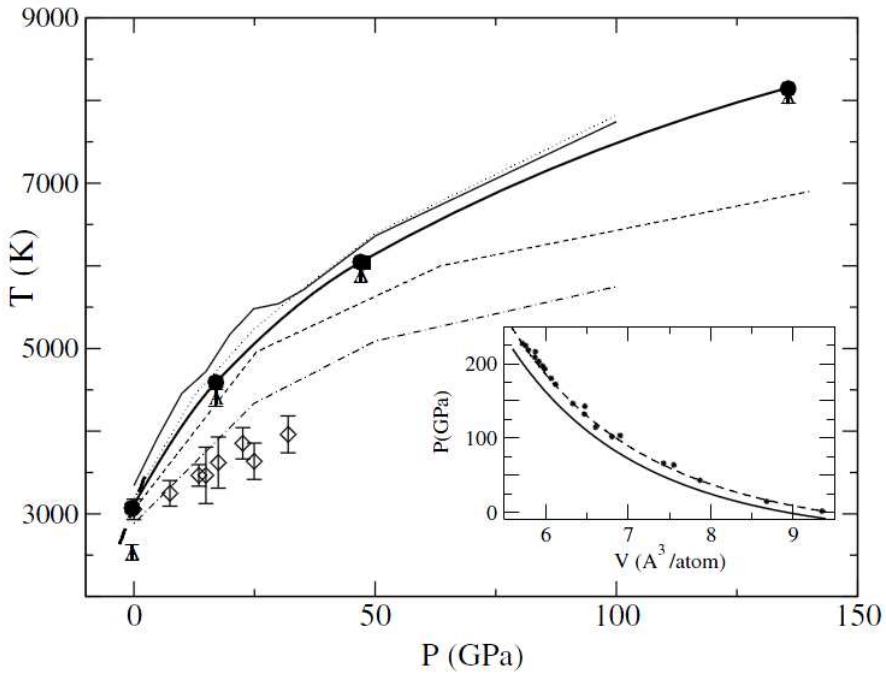

Figure 12: Comparisons of experimental and ab initio data for the Hugoniot and melting temperature of MgO, Alphe [37]. Solid squares, rectangles and solid lines represent ab initio calculations using 432 and 1024-atom cells. Triangles represent DFT-CGA calculations and open diamonds denote the experimental data.

The above discussions have focused on properties of single-component systems. Mixture or 'solution' rules are required to model multi-component systems. For solids and liquids, the solution rules may be classified into three categories:

- Ideal solution
- Regular solution
- Non-regular solution

With the exception of CALPHAD-based codes, equilibrium codes do not usually include any solution rules in their calculations. This implies that each component has its own melting temperature and is not affected by the presence of any other component. Due to the development of CALPHAD codes, which began in the 1970's, considerable work has been done on the formulation of solution rules for different types of solid crystal structures. Comprehensive descriptions of this work may be found in the books by Saunders and Miodownik [38] and by Hillert [39].

4.6.1 Gibbs Energy of Mixing

Solution rules are introduced into an equilibrium calculation through the addition of a mixing energy to the overall Gibbs energy to be minimized. For a system containing species A and B, the total Gibbs energy is then given by:

$$G_{Total} = x_A G_A + x_B G_B + G_{mix}$$

where G_{mix} is the Gibbs energy of mixing.

Ideal Solution

An ideal solution simply accounts for the increase in configurational entropy during mixing and assumes no attractive or repulsive forces between the atoms of the two different components, A and B. In this case, the Gibbs energy of mixing is given by:

$$G_{mix}^{ideal} = RT(x_A ln x_A + x_B ln x_B)$$

It can be seen from the above equation that an ideal solution model does not require any additional thermodynamic data beyond that for the individual components, A and B.

Regular and Non-Regular Solution

When the attraction and repulsion between components are considered, an additional 'excess energy' , G_{mix}^{xs} is introduced and added to the ideal solution contribution. In this case,

$$G_{mix} = G_{mix}^{ideal} + G_{mix}^{xs}$$

For a regular solution, the excess energy is given by:

$$G_{mix}^{xs} = x_A x_B \Omega$$

where Ω is positive or negative for repulsive or attractive potentials respectively. Different values of Ω must be obtained for liquid and solid solutions to construct a phase diagram. As illustrated in Figure 13 from Pelton [40], the sign and magnitude of these values play an important role in determining the topology of the phase diagram. For non-regular solutions, additional terms are added to the ideal solution mixing energy using a power series of interaction terms. The temperature-concentration (T-C) diagrams are also dependent on the system pressure. Figures 14 and 15 display computed and experimental phase diagrams for Al-Si (Brosh et al. [14]) and Ag-Cu (Gheribi et al. [41]) at ambient and elevated pressures.

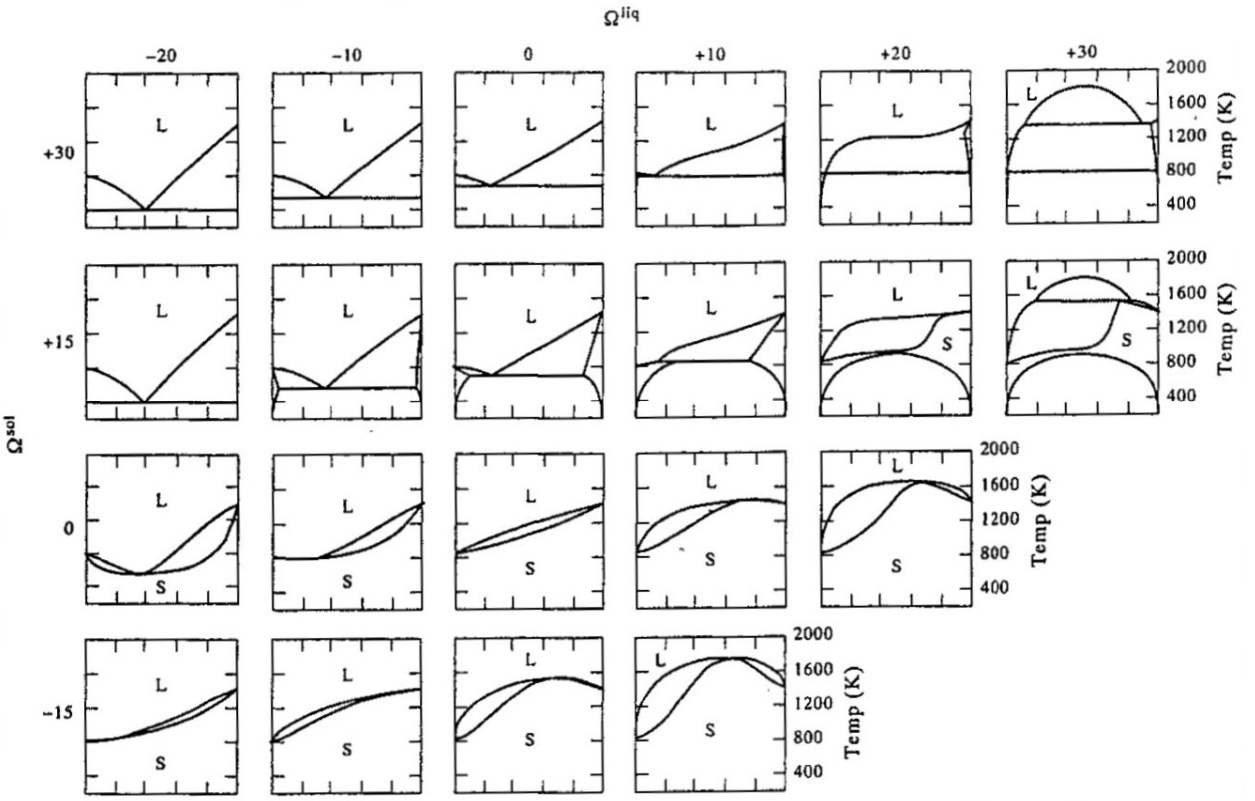

Figure 13: Different phase diagram topologies as a function of liquid and solid excess energy [40]

5. Equilibrium Calculations for SHS Systems of Interest

Several systems have been proposed for SHS combustion [42]. The purpose of this section is to present some sample equilibrium calculations using various equilibrium codes. These include CERV [1], FactSage [43], CEA [44] and Thermo [42,45]. Systems such as Ti-Si and Ti-B are not only energetic but remain essentially gasless during combustion even at ambient atmospheric pressure. 'Thermite' reactions involving F_2O_3-Al or MoO_3-Al can generate significant amounts of gaseous products when burned at 1 atm. However, such systems may indeed be gasless at detonation pressures. Thermite systems offer the advantage that the reactants and products have been extensively studied at high pressure. The discussion below presents phase diagrams and equilibrium constant pressure combustion calculations for these two types of systems.

5.1 Ti-Si and Ti-B System

5.1.1 Ti-Si System

Figure 16 presents Ti-Si phase diagrams from Massalski [46] and calculated using FactSage. The results are similar with the exception that FactSage combines the Ti_5Si_3 and Ti_5Si_4 regions into a solid solution of the two combustion products. It should also be noted that FactSage calculations use a liquid phase database that only contained the reactants Ti and Si. As

indicated in Figure 17, FactSage can also compute the gas phases at higher temperatures. FactSage was used to calculate the constant pressure combustion temperature as a function of concentration. The results are included with the phase diagram in Figure 18. Also shown, are results computed using the Thermo equilibrium code [42]. The main difference between the two calculations is that Thermo contains the liquid phase products TiSi and Ti_5Si_3, which are not available in the FactSage database. FactSage calculations indicate a maximum temperature for a stoichiometric composition for the reaction 3Ti + 5Si -> Ti_3Si_5. Finally, no results from CERV or CEA are displayed in the figure since the databases used by these codes to not contain any of the required combustion products in solid or liquid phases.

5.1.2 Ti-B System

The results of similar calculations are provided below for the Ti-B system. As seen from Fig. 19, the FactSage phase diagram differs from that from Massalski in the central region of the diagram due to a 'B2M' prototype solution model used in that region. Figure 20 displays the gas regimes that occur at higher temperatures. Constant pressure combustion temperatures are displayed in Fig. 21 based on calculations performed using FactSage, Thermo and CERV. The calculations using FactSage and Thermo are more consistent than for the Ti-Si system since the databases used by both codes contain the dominant combustion products TiB (solid), TiB_2(solid) and TiB_2(liquid). One important difference between the two calculations is that Thermo predicts a peak temperature for the (1Ti + 1B) system (boron mole fraction, 0.5), whereas FactSage indicates a peak temperature for the (1Ti + 2B) system (boron mole fraction, 0.667). CERV and CEA use a similar database that also contain the desired phases of the TiB and TiB_2 combustion products. However, CERV only converged for two points yielding significantly lower temperatures than FactSage and Thermo. Finally, CEA calculations did not converge for this system. This may be due to the fact that the combustion for this system is gasless. It is possible that better convergence could have been obtained by arbitrarily adding a small mole fraction of inert gas in the reactants.

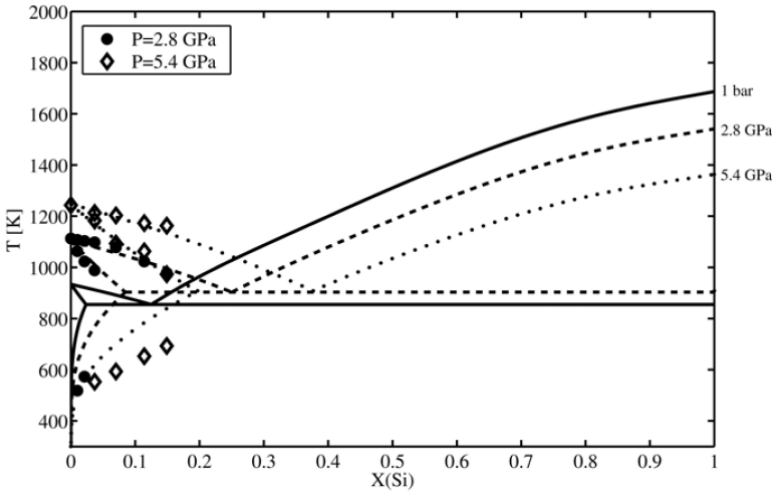

Figure 14: Phase diagrams for Al-Si system at different pressures [14]

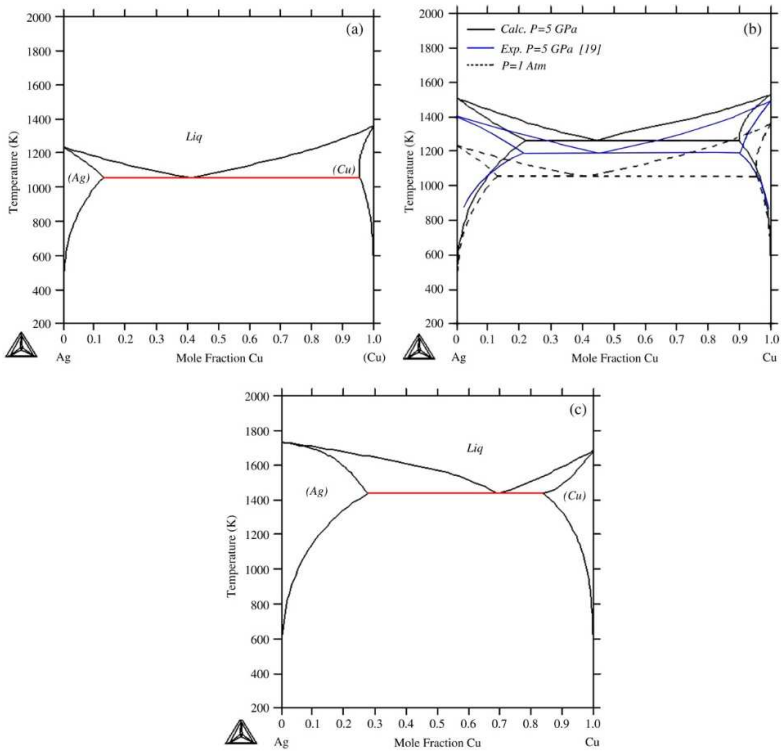

Figure 15: Phase diagrams for Ag-Cu system at different pressures [41]. a) standard pressure, b) 5 GPa and c) 10 GPa.

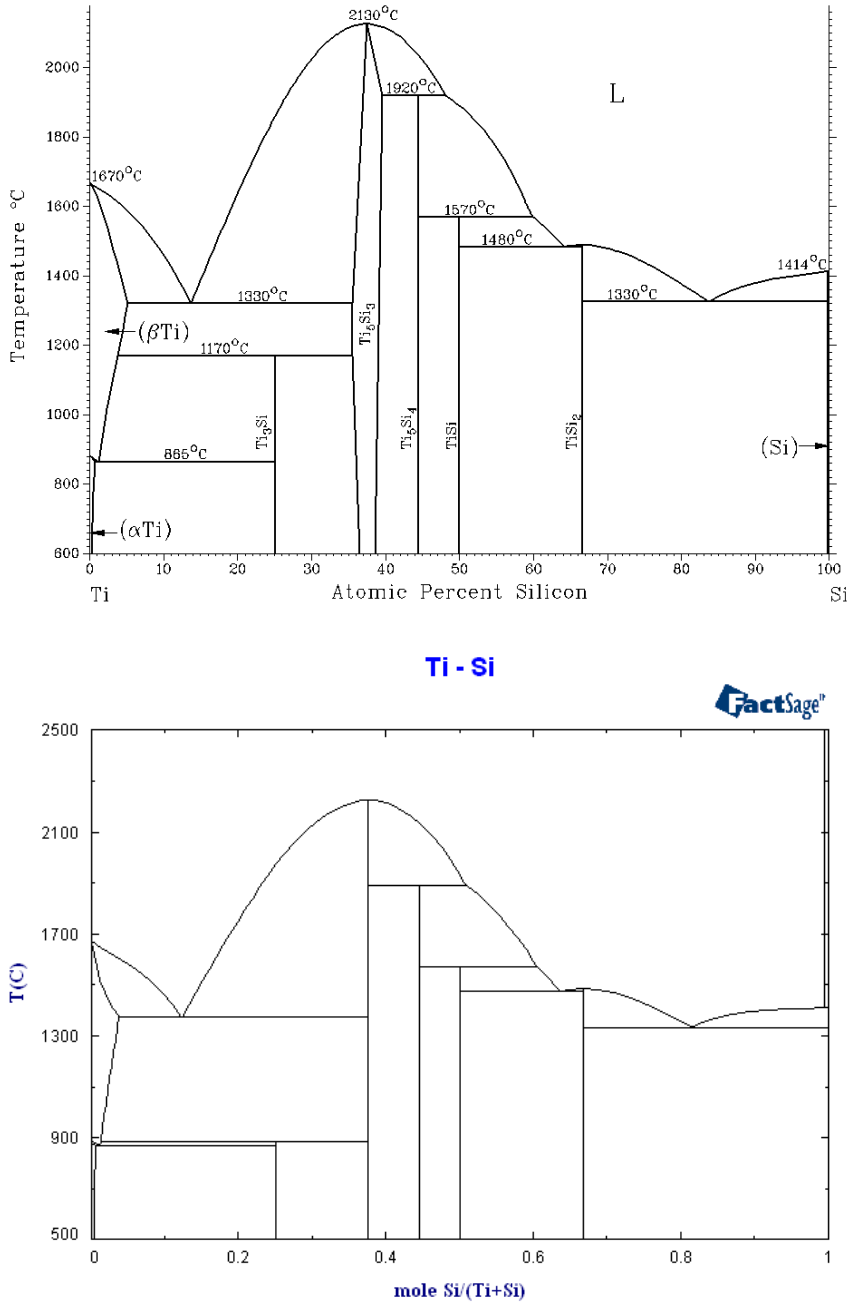

Figure 16: Phase diagrams for Ti-Si system: Massalski [46] (top), FactSage (bottom).

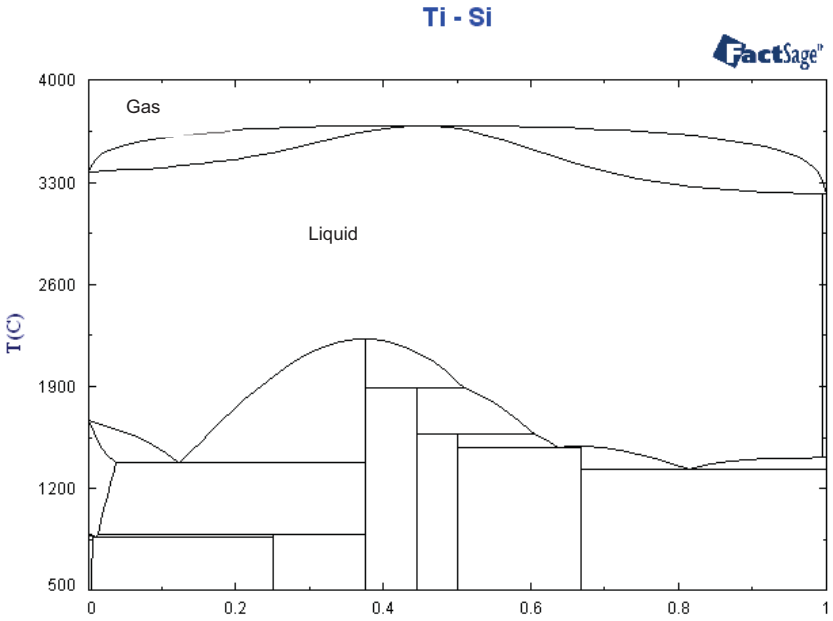

Figure 17: Phase diagrams for Ti-Si system showing gas phase at higher temperatures (computed using FactSage).

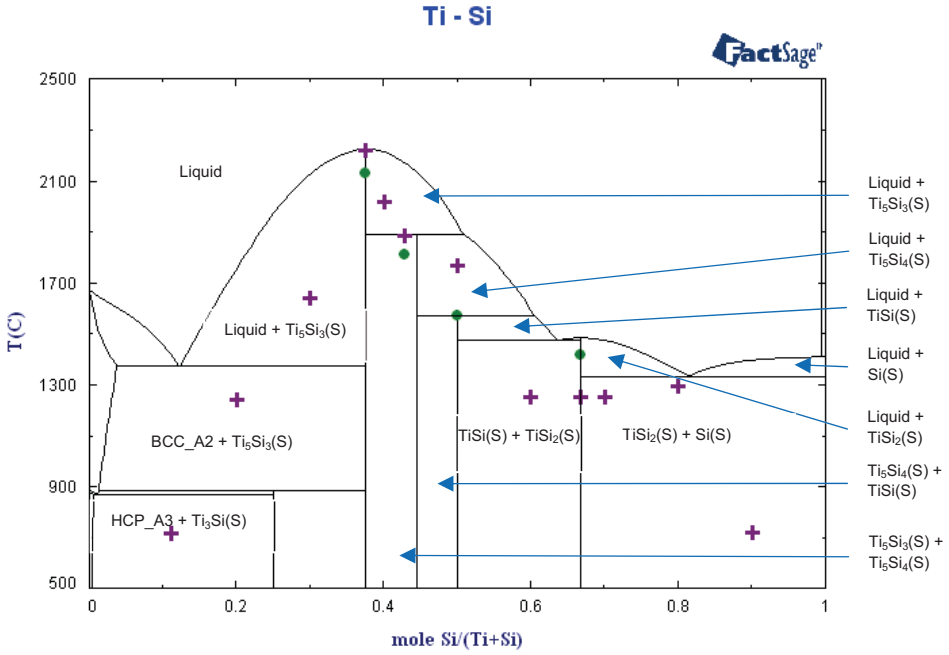

Figure 18: Comparison of constant pressure combustion temperatures using FactSage (+) and Thermo (o) [42].

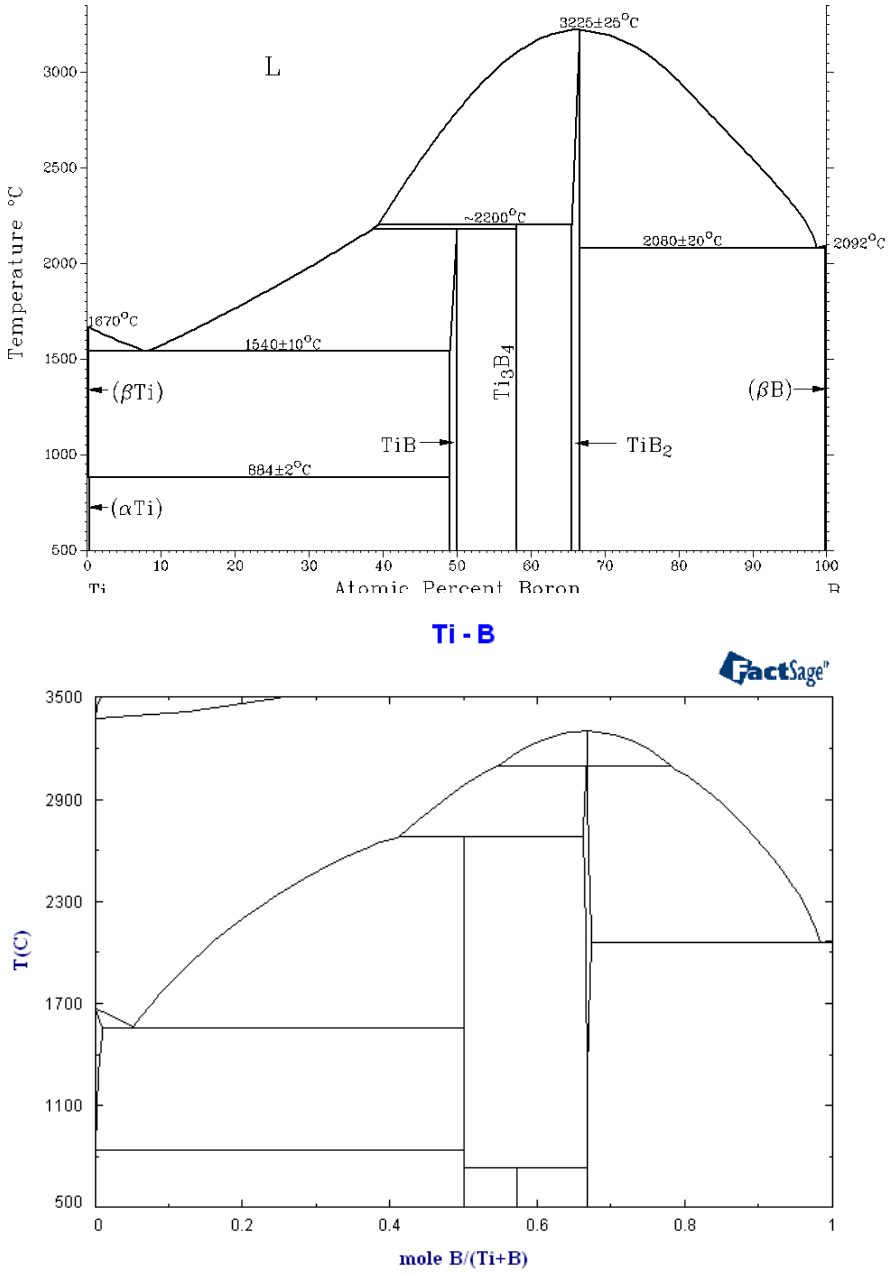

Figure 19: Phase diagrams for Ti-B system: Massalski [46] (top), FactSage (bottom).

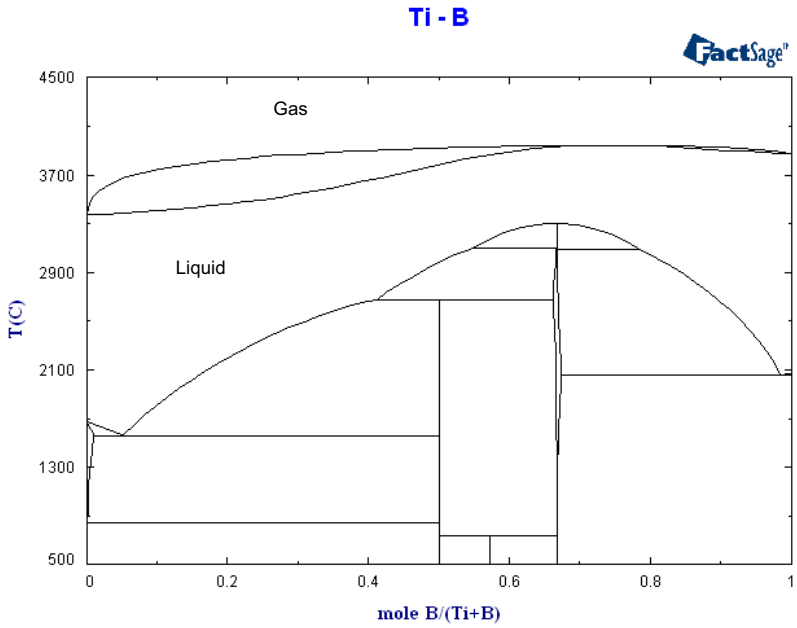

Figure 20: Phase diagrams for Ti-B system showing gas phase at higher temperatures (computed using FactSage).

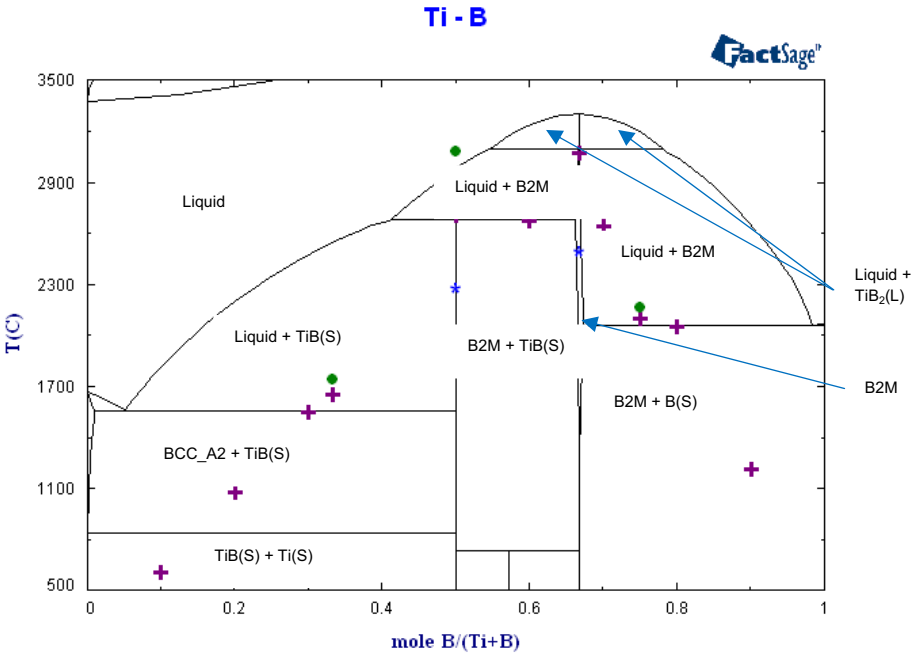

Figure 21: Comparison of FactSage (+), Thermo [42] (o) and CERV (*) constant pressure combustion temperatures for Ti-B system.

5.2 Thermite Systems

5.2.1 MoO_3-Al System

Constant pressure combustion properties for the MoO_3-Al system were calculated using FactSage, CERV and CEA. The results are included in a phase diagram computed using FactSage (Fig 22). The FactSage calculations indicate that the combustion temperature peaks for a stoichiometric mixture corresponding to the reaction MoO_3 + 2 Al -> Mo + Al_2O_3. The results from the CERV calculations are very different and suggest a strongly exothermic decomposition combustion for pure MoO_3, which is not observed in the FactSage calculations. This is due to the fact that the CERV database does not include the required solid phase of MoO3 in its thermodynamic database. FactFage calculations indicate that, for temperatures below 1060°C, significant concentrations of condensed MoO_3 remain in the products for Al mole fractions lower than 0.4. CEA had considerable difficulty converging to results unless specific condensed species were omitted or included based on the FactSage calculations. When this was done, CEA provided similar results as FactSage for the cases where CEA converged. A similar comparison was not possible with CERV since the code does not currently provide the option to include or omit specific species or phases from the calculations. Finally, no Thermo results have been reported for thermite systems in ref [42].

5.2.2 Fe_2O_3-Al System

Figure 23 provides comparisons between FactSage and CERV calculations for the Fe_2O_3-Al system with results that are qualitatively very similar to those for the MoO_3-Al system. The Fe_2O_3-Al system results in lower combustion temperatures with CERV once again predicting high combustion temperatures for pure Fe_2O_3 due to the lack of thermodynamic data for the condensed phases of this oxide. It can be noted that the phase diagram computed by FactSage is not totally complete. It is not clear at this time whether this is a computational or graphical problem.

5.3 Al-O_2 System

Due to the discrepancies observed above for thermite systems, calculations were performed for the simple Al-O_2 system to determine if the various code/database combinations computed different results for aluminium oxidation. Figure 24 displays constant pressure combustion temperatures computed with FactSage, CERV and CEA. As in previous cases, the phase diagram was calculated using FactSage. CERV calculations did not converge for very low or high concentrations of O_2 due to the fact that the code encounters convergence problems at temperatures below approximately 500 °C. With the exception of one point, where the CERV value is slightly higher, the results obtained from the three codes are very similar. This would indicate that the main differences observed for the thermite system are related to reactions that involve Mo or Fe.

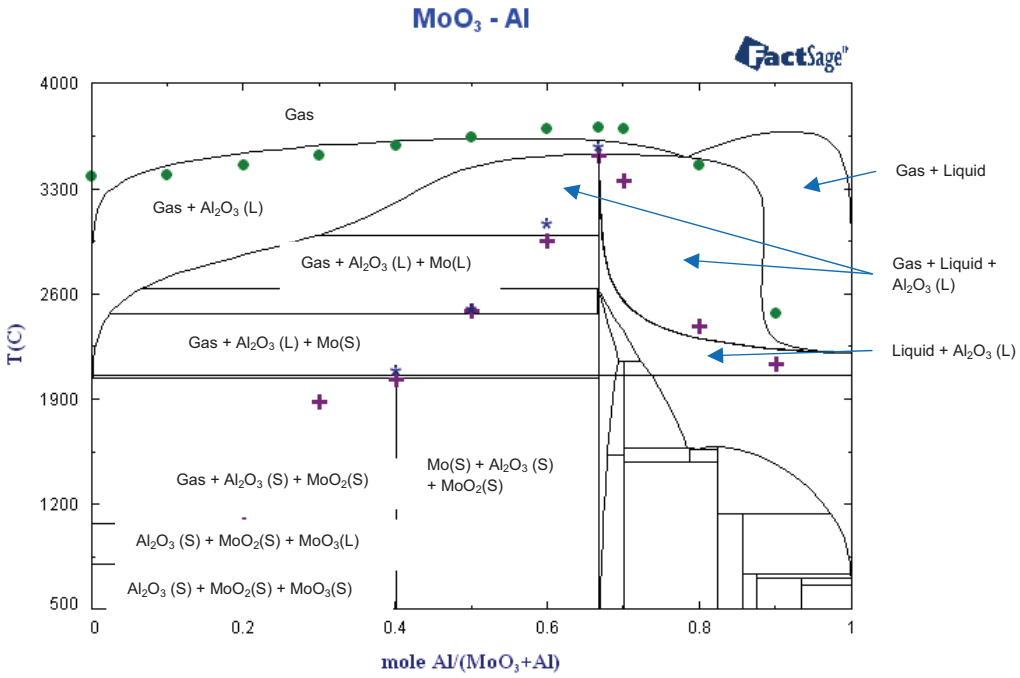

Figure 22: Comparison of FactSage (+) , CERV (o) and CEA (*) calculations for the constant pressure combustion temperatures for the MoO_3-Al system.

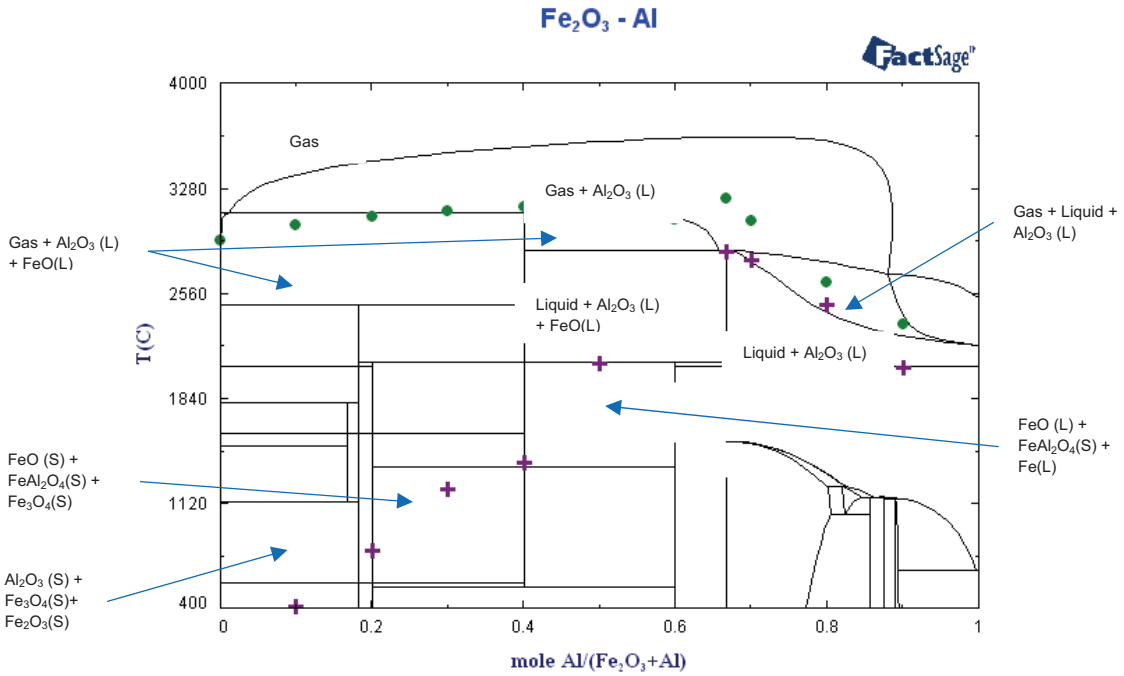

Figure 23: Comparison of FactSage (+) and CERV (o) calculations for the constant pressure combustion temperatures for the Fe_2O_3-Al system.

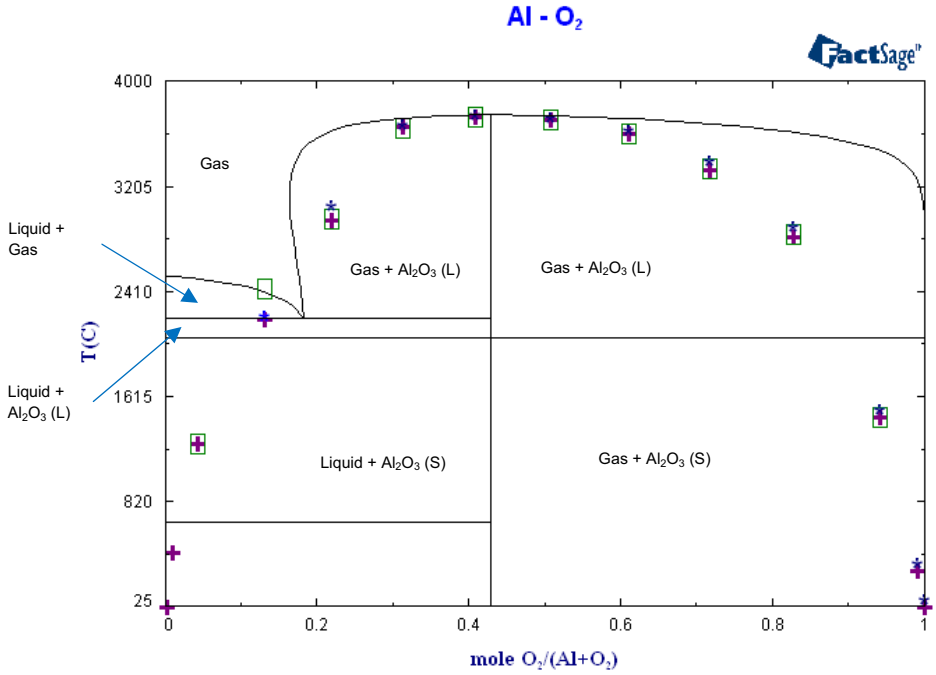

Figure 24: Comparison of FactSage (+) and CERV (□) and CEA (*) constant pressure combustion temperatures for the Al-O_2 system.

5.4 General Observations on the Various Codes used for Calculations

Comparisons between different equilibrium codes remain difficult due to the fact that they typically use not only different solvers, but also different databases for the thermodynamic properties. In spite of this, the calculations presented above do shed some light on the overall robustness of the code.

The CALPHAD-based FactSage code solver seems to be very robust as no convergence problems were encountered during the equilibrium calculations performed in this study. Such solver performance is probably not surprising since CALPHAD codes are expected to calculate complex phase diagrams. This requires good convergence capabilities for a wide range of component concentrations and thermodynamic states. FactSage does not have a complete database for the condensed phase combustion products. In particular, limited data is available for the molar volumes, which are of particular importance in assessing SHS detonation feasibility. The code also does not currently support calculations for detonation or for constant volume combustion, where both the volume and internal energy is kept constant. It is possible that such capabilities could be implemented through the ChemApp software library [47], which provides a C or FORTRAN interface to the chemical equilibrium solver and database.

Although CERV and CEA use a very similar database, CERV appears to offer superior convergence performance, except for calculations involving low temperatures below 500 °C. Both CERV and CEA had difficulties with calculations involving the Ti-B system and did not

have the required condensed phase combustion products in their database to compute the Ti-Si system. Although CEA has been used successfully for a wide range of gaseous systems, it often encounters matrix singularities and fails to converge for systems involving condensed species. When convergence is actually achieved, the user is often required to insert or omit selected species. This procedure is not only tedious but can require some prior knowledge of the solution, which diminishes the code's predictive capabilities.

Very little is known concerning the solver and database used by the Thermo code. Based on the results presented in reference [42], the code seems to include thermodynamic data for a wide range of gaseous and condensed species. Since final system densities are not reported in this reference, Thermo may also lack the molar volume data required for such a calculation. As with FactSage, Thermo does not support detonation calculations.

5.5 Thermodynamic Data Required for Future Calculations

The eventual computation of detonation properties for SHS systems will require suitable data for the:

1. Thermodynamic properties and molar volume for the relevant phases,
2. Equation of state parameters,
3. Melting temperature dependence on pressure.

As previously stated, the pressure range of interest for SHS detonation is of the order of 5-50 GPa, depending on the mixture components and the system porosity. Some of this data is available for monatomic metal elements and for minerals of particular interest to geophysics. As can be seen from references 48-64, numerous experimental and numerical studies have been performed for materials relevant to the systems discussed in this report. Most of the available data, however, are mainly relevant to thermite systems due to the relevance of the reactants and combustion products to earth sciences. These experimental data are obtained through the combined use of a Diamond Anvil Cell (DAC) and X-Ray diffraction. The most promising theoretical work has been performed using ab initio calculations based on the Density Functional Theory (DFT). Key laboratories for these studies include the earth science groups at the Uppsala University (Sweden) for the experimental work, and the University College London (UK) for numerical studies. In addition to the listed publications in the reference section of this report, these institutions represent a potentially good source of information concerning available data for some of the SHS systems of interest. The first priority should focus on obtaining the data required to determine the volume expansion after constant pressure combustion. This is important since a positive volume expansion is required for SHS detonation.

6. Incorporation of Condensed Species Equation of State in CERV

6.1 General Considerations

As noted in Section 2 of this report, CERV can now model a variety of thermodynamic states and processes, with post-processing capabilities to construct plots in the P-V plane. This has been possible through the following activities:

1. Re-structuring of the code by UTIAS to provide a library of subroutines for a variety of problem types (TP, TV, HP and UV),

2. The use of the above routines by TimeScales Scientific Ltd. to construct new subroutines for additional problem types (PV, isentrope, sound speed, Hugoniot and detonation),

3. The development by TimeScales of a post processor program to create the required plots in the P-V plane.

Section 2.3 of this report summarizes some of the current CERV limitations. The purpose of this section is to discuss these limitations in greater detail, with the aim of prioritizing future code development activities, which include:

1. Addition of physical models,
2. Improvements to the code solver to enhance convergence characteristics,
3. Expansion of the database.

6.2 Addition of Physical Models

The modelling of SHS detonations will require model improvements for condensed and gaseous phases. Since one of the main objective of the SHS detonation research is to achieve gasless combustion, the condensed phase models are of greater importance and will be discussed first.

6.2.1 Condensed Phase Models

The main requirements for improvements to the condensed phase calculations in CERV include models for:

1. Compressibility,
2. Thermal expansion,
3. Dependence of melting temperature on pressure,
4. Solid and liquid phase molar volumes,
5. Solution modelling.

As discussed in Sections 4.2 and 4.3 of this report, the first two requirements involve the inclusion of an equation of state that can accommodate "cold " isothermal compression along with thermal expansion. Various models have been developed for isothermal compression ranging from a simple bulk modulus model to more detailed Birch-Murnaghan, logarithmic and Vinet models that involve additional parameters such as the pressure derivative of the bulk modulus. The thermal expansion is introduced through a Mie-Gruneisen equation where a suitable Gruneisen coefficient must be chosen. This report provides various thermodynamic relations and approximations that facilitate the estimate of some of the relevant parameters.

Assuming that more complex equations of state do not introduce any specific convergence problems, the introduction of increasingly more accurate models should not pose any major difficulties. One consideration is that CERV currently uses state variable derivatives for its minimization of the Gibbs energy. If the condensed species EOS are not easily differentiated,

suitable differentiable curve fits to the EOS could be developed. Alternatively, a lower order minimization process, not requiring derivatives, could be used.

The successful modeling of SHS detonations requires the ability to incorporate different molar volumes for solid and condensed phases, along with the accommodation of a melting temperature that is dependent on pressure. Whereas the first requirement depends of the availability of suitable experimental or ab initio calculation data, the second requirement can be accommodated through one of many available melting models. The theory of Lindemann and Gilvarry theory has been particularly successful in modeling monatomic metals. Although the modelling of polyatomic combustion products is more challenging, promising results have been obtained for such systems using the more recent model by Wang et al [29] and by applying more fundamental ab initio methods.

An accurate modelling of a SHS mixture through a range of compositions requires the introduction of solution models of the type commonly used in CALPHAD codes. Due to the level of effort involved, it would not be realistic to introduce full solution modelling capabilities in CERV. Nevertheless, an ideal solution model could be introduced relatively easily based on the discussion in Section 4.6 in this report. Limited non-ideal solution modelling capabilities could possibly be introduced for a very specific region of the phase diagram by fitting solid and liquid excess energies to obtain results that are consistent with phase diagram data obtained from experiments or from separate CALPHAD code calculations.

6.2.2 Gaseous Phase Models

As previously noted, CERV currently uses a virial expansion, which is probably not suited for the very high pressures generated by SHS detonations. JCZ equations of state, initially developed for condensed explosives, would be more suitable to accommodate such pressures. This limitation may not be serious if the SHS combustion is gasless at atmospheric pressure, or becomes gasless at the elevated detonation pressure. In the latter case, the gases would only be produced when the combustion products have been expanded to a lower pressure where gases are eventually produced. For most systems of interest, the pressure where this occurs may be low enough for the virial expansion to remain valid. In this case, the only requirement for the EOS is to be reasonably well behaved at very high pressures to prevent solver convergence failure and avoid the calculation of a totally incorrect state. Finally, CERV currently assumes an ideal gaseous mixture and therefore neglects the cross-terms for the virial EOS coefficients. Once again, considering that the main interest is in gasless combustion, this limitation may not be very significant.

6.3 Improvements to Solver

As previously noted, CERV does not currently provide the same level of convergence robustness as CALPHAD-based codes such as FactSage. CERV also encounters convergence difficulties at lower temperatures. This not only causes problems for systems with relatively low exothermicity, but prevents calculations of the 'frozen' Hugoniot for the unreacted material. The code also encounters difficulties for some systems such as, Ti-B, where converged results are only obtained for a narrow range of concentrations. The underlying reasons for these convergence problems need to be identified to allow suitable remedies to be implemented.

6.4 Expansion to Database

CERV is currently based on a NASA database that is similar to that used by CEA. This database has been developed for gases and incompressible condensed phases. As indicated in the calculations performed for this report, the database lacks the appropriate condensed phase combustion products to model the Ti-Si system or the Fe_2O_3 and MoO_3 reactants for thermite systems. Although the database provides an entry field for the liquid and solid phase densities, the actual data for the values are lacking for the systems of interest. Finally, an additional database is required to store equation of state parameters for the condensed phases as well as the pressure dependence of the melting temperature. One important factor to keep in mind is the requirement that new models and data must be introduced into the equilibrium code in a way that ensures that the overall thermodynamic data is self consistent. Finally, in order to allow comparisons with other codes and databases, CERV should allow the user the option to add and remove selected species and phases.

6.5 Summary of Requirements and Level of Importance

Requirements	Level of Importance	ID
Physical Models		
Condensed Phase		
Compressibility	A	P1
Thermal expansion	A	P2
Melting temperature as a function of pressure	A	P3
Solid and liquid phase molar volume	A	P4
Solution modelling (ideal and non-ideal)	C	P5
Gas Phase		
JCZ equation of state	C	P6
Non-ideal mixture	D	P7
Database Expansion		
Thermo data for condensed phases of all reactants and products	A	D1
Compressibility and thermal expansion data	A	D2
Melting temperature and molar volumes	A	D3
Solution excess energy parameters	C	D4
Allow insertion and removal of specie/phase	B	D5
Solver Capabilities		
Improve convergence for low temperature	B	S1
Improve convergence for range of SHS systems	A	S2
Improve solver speed	D	S3
Consolidate Gibbs energy minimization into a separate function	B	S4

Based on the above discussions, the table above summarizes the overall CERV development requirements and assigns a level of importance from A to D, with A being the most important. The table also includes some requirements that are specific to the equilibrium solver such as improving the convergence and speed, and separating sections of the code that are repeated in the various subroutines. These code sections could be consolidated into separate subroutines. Sections that could be consolidated include those used for Gibbs energy minimization and root solving.

6.6 Structure of CERV Code

The current CERV code is based on a library of subroutines that are used for different types of problems. The main subroutines, where equilibrium concentrations are calculated, correspond to those associated with the TP, TV, UV and HP problems. These subroutines access the database and minimize the Gibbs energy. The additional subroutines developed by TimeScales use these subroutines rather than directly call the equilibrium solver. The latter subroutines will therefore not be greatly impacted by changes in the database or the equilibrium solver. The overall structure of the equilibrium code is displayed below for the subroutine responsible for TP calculations.

Subroutine tp_problem

- ***scalnatm:*** scale the number of atoms
- ***select:*** select product species
    - ***inisiep:*** initialize collision diameters and attraction potentials
        - ***step:s*** estimate and initialize collision diameters and attraction potentials
- ***wmconv:*** convert weight percentages of reactants to mole percentages
    - ***ludcmp***
    - ***lubksb***
- ***transtemp:*** calculate transition temperatures for condensed species pairs
    - dmu0
- ***du:*** calculate the difference in internal energy of reactants and products
    - ***sort:*** sort array in descending order
    - ***stoichi*** :matrix reduction
    - ***ortho:*** determine independence among a set of vectors
    - ***vir_coe:*** calculate virial coefficients for ideal mixture
    - ***con*** : calculate equilibrium composition using the modified virial equation of state
        - ***chmpot:*** calculate chemical potentials of gaseous species (ideal mixture)
            - ***pres:*** calculate pressure
                - ***dv*** : calculate gaseous and condensed species volumes
        - ***kalpa:*** determine step size for positive mole numbers
        - ***lambda:*** determine step size to find minimum Gibbs energy
            - ***chmpot:*** calculate chemical potentials of gaseous species only
- ***melt:*** calculate equilibrium composition at transition temperature
    - ***ortho:*** determine independence among a set of vectors
    - ***stoichi*** :matrix reduction
    - ***intlx:*** calculate initial mole numbers of gaseous and condensed species (minimize Gibbs energy)
        - ***gg:*** calculate Gibbs energy
        - ***simplx:*** simplex method
        - ***stoichi*** :matrix reduction
    - ***gg:*** calculate Gibbs energy
    - ***sort:*** sort array in descending order

    - o ***vir_coe:*** calculate virial coefficients for ideal mixture
    - o ***ul***
- ***sort***

Not all of the subroutines/functions listed above are affected by the requirements listed in section 6.5. The table below identifies the subroutines that would be affected by the implementation of a required feature. This provides a partial insight into the level of effort required to address a requirement. With the exception of the requirement, D5, for species removal and addition, the requirements addressed in the table are limited to those involving the physical models. When a subroutine calls other subroutines, the requirements listed correspond to those that have not been addressed by the "children" subroutines lower in the hierarchy. This implies that all "parent" subroutines inherit the requirements of their children.

TP Problem Subroutine					**Requirements**
scatnatm					
select					D5
	inisiep				
		steps			
wmconv					
	ludcmp				
	lunksb				
transtemp					P3
du					
	sort				
	stoichi				
	ortho				
	vir_coe				P7
	con				
		chmpot			P1, P2, P5, P7
			pres		P1, P2, P6
				dv	
		kalpa			
		lambda			
			chmpot		P1, P2, P5, P7
melt					P3, P4
	ortho				
	stoichi				
	intlx				
		gg			P1, P2, P5, P7
		simplx			
		stoichi			
	gg				P1, P2, P5, P7
	sort				
	vir_coe				P7
	ul				
sort					

The next step in using the above table is to break down the various requirements and affected subroutines into more detail in order to identify particular software development tasks and determine the estimated level of effort required for their completion.

7. Summary and Proposed Approach

This report has summarized the current CERV capabilities and limitations and has identified possible models that could be added to the code for condensed and gaseous phase modelling. Particular attention has been given in the discussion to the implementation of suitable equations of state and melting models for condensed species along with databases for the model parameters. In order to assist in identifying and characterizing the CERV strengths and deficiencies, comparisons have been made with other codes for the constant pressure combustion temperatures of selected mixtures. The codes used for comparisons include FactSage, CEA and Thermo. The various codes have been applied to the Ti-Si and Ti-B systems and to the thermite systems, MoO_3-Al and Fe_2O_3-Al. Based on the models reviewed and the calculations performed, the CERV limitations have been summarized in terms of their level of importance to SHS modelling and the impact they may have on various sections of the CERV code.

The main CERV limitations involve the lack of suitable models to address the compressibility and thermal expansion of condensed species. These limitations can be addressed by implementing a suitable 'cold' isothermal compression model, such as the Birch-Murnaghan, Logarithmic or Vinet equations, supplemented by a thermal pressure adjustment trough the Mie-Gruneisen equation. This report provides various relations and references to perform initial estimates for some of the coefficients in these equations. Additional information is also provided to estimate the dependence of the melting temperature on pressure. This information should be sufficient to initiate the required code development. More detailed EOS data will subsequently be obtained through the work of Ecole Polytechnique, who will identify the most promising SHS mixtures based on the expansion of the products following constant pressure combustion. More detailed high pressure calculations will then be performed based on available EOS and melting temperature data. For this purpose, this report has also identified references and institutions that could provide additional information for the required EOS and melting data. The institutions include the Uppsala University (Sweden), who have performed extensive experimental studies using a heated Diamond Anvil Cell (DAC) with X-Ray diffraction, and the University College London (UK), who have been very active in ab initio calculations.

Extension to the CERV code capabilities will require a systematic evaluation of the code to plan a development strategy. For this purpose, this report has listed the various requirements and assigned appropriate levels of importance. It has also related the various requirements to different sections of the code. The next step is to combine the levels of importance and effort in order to develop a prioritised list of work items with estimated dates of completion.

8. References

1. Wong, F.C.H., Gottlieb, J.J, and Lussier, L-S, "Chemical Equilibrium Analysis of Combustion Products at Constant Volume", Defence R&D, Canada - Valcartier, Technical Report, DRDC Valcartier TR 2003-375, 2003-12-22. 2003.

2. Van Wylen, G.J. and Sonntag, R.E., "Fundamentals of Classic Thermodynamics" John Wiley & Sons, 1985.

3. Mc Quarrie, D.A. ,"Statistical Mechanics", Harper & Row, 1976.

4. Hirschfelder, J.O., Curtiss, C.F., and Bird, R.B., "Molecular Theory of Gases and Liquids", Wiley, 1954.

5. Davis, W.C., "Shock Waves; Rarefaction Waves; Equations of State" from "Explosive Effects and Applications" J.A. Zukas and W.P. Walters (Ed.), Springer, 1997.

6. McGee, B.C., Hobbs, M.L. and Baer, M.R., "Exponential 6 Parameterization of the JCZ3-EOS", Sandia Report SAND98-1191, 1998.
http://prod.sandia.gov/techlib/access-control.cgi/1998/981191.pdf

7. Poling, B.E., Pausnitz, J.M. and O'Connell, J.P., "The Properties of Gases and Liquids", Fifth Edition, Chapter 5, McGraw-Hill, 2001.

8. Poirier, J-P, "Introduction to the Physics of the Earth's Interior", Cambridge University Press, 2000.

9. Anderson, O.L., "Equations of State of Solids for Geophysics and Ceramic Science", Oxford University Press, 1995.

10. Peiris, S.M. and Gump, J.G., "Equations of State and High Pressure Phases for Explosives" book chapter in "Static Compression of Energetic Materials", Ed. Suhithi M. Peiris and Gasper J. Piermarini, Springer, 2008.

11. Dattelbaum, D.M. and Stevens, L.L., "Equations of State of Binders and Related Polymers", book chapter in "Static Compression of Energetic Materials", Ed. Suhithi M. Peiris and Gasper J. Piermarini, Springer, 2008.

12. Grimwall, G., "Thermophysical Properties of Materials, Enlarged and Revised Edition", North-Holland, Elsevier, 1999.

13. Anderson, O.L., '"A Universal Thermal Equation of State", J. Geodynamics, Vol. 1, pp. 185-214, 1984.

14. Brosh, E., Makov, G. and Shneck, R.Z., "Application of CALPHAD to High Pressures", Computer Coupling of Phase Diagrams and Thermochemistry, Vol. 31, pp. 173-185, 2007.

15. Dubrovinsky, L.S. and Saxena, S.K., "Thermal Expansion of Periclase MgO and Tngsten W to melting Point, Phys, Chem. Miner., Vol. 24, pp. 547-550, 1997.

16. Chang, Y.A., "A Correlation of the Coefficients of Thermal Expansion of Metallic Solids with Temperature", The Journal of Physical Chemistry, Vol. 70, No. 4, , Notes, pp. 1310-1312, 1966.

17. Gheribi, A.E., Roussel, J.M. and Rogez, J., "Phenomenological Hugoniot Curves for Transition Metals up to 1 TPa. Journal of Physics, Condensed Matter, Vol. 19, 476218, pp. 1-9, 2007.

18. Fernandez, G.E., "A Debye-Gruneisen Thermal Correction to the Murnahan Equation of State of Solids", The Journal of Physics and Chemistry, Vol. 59, No. 6-7, pp. 867-870, 1998.

19. Vocadlo, L., Poirier, J.P. and Price, G.D., "Gruneisen Parameters and Isothermal Equations of State", The American Mineralogist, Vol. 85, No. 2, pp. 390-395, 2000.

20. Segletes, S.B., "Thermodynamic Relations along Principal Hugoniot", Shock Waves, Vol. 8, pp. 361-366, 1998.

21. Schlosser, H., Vinet, P. and Ferrante, J., "Pressure Dependence of the Melting Temperatures of Metals", Physical Review B, Vol. 40, No. 9, pp. 5929-5935, 1989.

22. Lindemann, F.A., "Uber die Berechnung molekularer Eigenfrequenzen", Physikalisches Zeitsch, Vol. 11, pp. 609-612, 1910.

23. Gilvarry, J.J., "The Lindemann and Gruneisen Laws", Phys. Rev., Vol 102, pp. 308-316, 1956.

24. Fang, Z-H and Chen, L-R, "A Simplified Treatment to Calculate the Melting Temperature of metals Under High Pressure", Journal of Physics Condensed Matter, Vol. 6, pp. 6937-6940, 1994.

25. Lennard-Jones, J.E. and Devonshire, A.F., "A Theory of Disorder in Solids and Liquids and the Process of Melting", Proceedings of the Royal Society London, A Vol. 170, pp. 464-484, 1939.

26. Shen, G., Lazor, P., "Measurement of Melting Temperatures of some Minerals under Lower Mantle Pressures", J. Geophys. Res., 100, 17699-17713, 1995.

27. Shen G, Lazor P, Saxena SK, "Melting of Wustite and Iron up to Pressures of 600 kbar", Phys Chem Minerals, 20, 91-96, 1993.

28. Wang, Z., Lazor, P., Saxena, S.K., "A New empirical Method for Estimating the High Pressure Melting Temperatures of Solids, NaCl as an Example", High Temp. High Press., 33, 357-363, 2001.

29. Wang, Z., Lazor, P., Saxena, S.K., "The Analysis of High pPessure Melting Temperature Dependence of Thermodynamic Parameters of Solids", Materials Letters, 49, 287-293, 2001.

30. Wang Z., Lazor P., Saxena S.K., "A Simple Model for Assessing the High Pressure Melting of Metals: Nickel, Aluminium and Platinum", Physica B, 298, 408-416, 2001.

31. Oriani, R.A., "The Entropies of Melting Metals", J. Chem. Phys., Vol. 19, pp. 93.97, 1951.

32. Tallon, J.L., "The Entropy Change on Melting of Simple Substances", Physics Letters, Vol. 76A, 1980.

33. Wallace, D.C., "Melting of Elements", Proceedings of the Royal Society London, A, Vol. 433, pp. 631-661, 1991.

34. Cramer, C.J., "Computational Chemistry", Theories and Models", Second Edition, Wiley, 2004.

35. Cazorla, C., Gillan, M.J., Taioli, S. and Alphe, D, "Melting Curve and Hugoniot of Molybdenum up to 400 GPa by ab initio simulations", Journal of Physisc: Conference Series, Vol. 121, 012009, pp. 1-8, 2008.

36. Alfe, D., Vocadlo, L., Price, G.D. and Price, M.J., "Melting Curve of Materials: Theory Versus Experiments", Journal of Physics: Condensed Matter, Vol. 16, pp. S973-S982, 2004.

37. Alfe, D., "Melting Curve of MgO from First-Principles Simulations", Physical Review Letters, Vol 94, No. 23, pp 235701-1 - 235701-4, 2005.

38. Saunders, N. and Miodownik, A.P., "CALPHAD, Calculation of Phase Diagrams, A Comprehensive Guide", Permagon, 1998.

39. Hillert, Mats, "Phase Equilibria, Phase Diagrams and Phase Transformations, Their Thermodynamic Basis", Second Edition, Cambridge University Press, 2008.

40. Pelton, A.D. in Physical Metallurgy, 3rd Edition, eds Cahn, R.W. and Haasen, P., ElsevierScience, Amsterdam, p. 328, 1983.

41. Gheribi, A.E., Rogez, J., Marinelli, F., Mathieu, J.C. and Record, M.C., "Introduction of Pressure in Binary Phase Diagram Calculations. Applications to the Ag-Cu System", Computer Coupling of Phase Diagram and Thermochemistry, Vol. (31), pp. 380-389, 2007.

42. "Assessment of Self-Propagating High Temperature Synthesis (SHS), Final Report for Work Carried out Under Contract No. W7702-5-R544/01-XSG", ZND Inc, March, 31, 1998.

43. FactSage, www.factsage.com, www.crct.polymtl.ca/factsage/fs_general.php

44. CEA and CEAGUI www.grc.nasa.gov/WWW/CEAWeb/ceaWhat.htm

45. Merzhanov, A.G., Int. J. SHS 2, pp. 133-156.

46. Massalski, T.B., "Binary Alloy Phase Diagrams, Second Edition, Plus Updates, Version 1", ASM International, 1996.

47. ChemApp Library, http://gttserv.lth.rwth-aachen.de/~cg/Software/ChemApp/IndexFrame.htm

48. Dubrovinsky, L.S., Saxena, S.K. and Lazor, P., "High-Presure and High-Temperature in Situ X-Ray Diffraction Study of Iron and Corundum to 68 GPa using Internally Heated Diamond Anvil Cell", Phys. Chem. Minerals, Vol. 25, pp. 434-441, 1998.

49. Dubrovinsky, L.S. and Saxena, S.K., "Iron at Extreme Conditions: in situ X-ray sSudy of P-V-T Relations in Internally Heated Diamond Anvil Cell and Modelling of Interatomic Potential of Iron", Petrology, Vol. 6, pp. 535-545, 1998.

50. Saxena, S.K. and Dubrovinski, L.S., "Thermodynamics of Iron Phases at High Pressures and Temperatures. Properties of earth and Planetary Materials at High Pressure and Temperature", Geophysical Monograph, Vol. 101, pp. 271-279, 1998.

51. Dubrovinskaia, N.A., Dubrovinsky, L.S., Karlsson, A., Saxena, S.K. and Sundman, B. "Experimental Study of Thermal Expansion and Phase Transformations in Iron-Rich Fe-Al Alloys", CALPHAD, Vol. 23, No. 1, pp. 69-84, 1999.

52. Dubrovinsky, L.S., Dubrovinskaia, N.A., Saxena, S.K., Rekhi, S. and Le Bihan, T., "Aggregate Shear Moduli of Iron up to 90 GPa and 1100 K, "Journal of Alloys and Compounds, Vol 297, pp. 156-161, 2000.

53. Dubrovinskaia, N.A., Dubrovinsky, L.S., Saxena, S.K., Ahuja, R. and Sundman, B., "High Pressure Study of Titanium Carbide", Journal of Allys and Compounds, Vol 289, pp. 24-27, 1999.

54. Dubrovinski, L.S., Saxena, S.K., Tutti, F., Rekhi, S. and LeBehan, T., "In Situ X-Ray Study of Thermal Expansion and Phase Transition of Iron at Multimegabar Pressure", Physical Review Letters, Vol. 54, issue, 8, pp. 1720-1723, 2000.

55. Andrault, D., Morard G., Bolfan-Casanova N., Ohtaka O., Fukui H., Arima H., Guignot N., Funakoshi K., Lazor P., Mezouar M., Study of Partial Melting at High Pressure Using in situ X-ray Diffraction", High Pressure Research, 26, 267-276, 2006.

56. Lazor P., "Temperature Measurement in a Laser-Heated DAC", Proceedings from International Symposium on Advanced Materials: Ultra-High Pressure Research (ISAM 2001), NIRIM, Tsukuba, Japan, 45-46, 2001.

57. Lazor, P., Saxena, S.K., Dubrovinsky, L.S., Weber, H.P., Le Bihan, T., "Synchotron X-ray Diffraction of Iron under High Pressure and Temperature", Science and Technology of High Pressure, Proceedings of AIRAPT-17, Honolulu, Hawaii, 25-30 July 1999, 1059-1062, 2000.

58. Dubrovinsky, L.S., Lazor, P., Saxena, S.K., Häggkvist, P., Weber, H.-P., Le Bihan, T., "Study of Laser Heated iron using Third Generation Synchrotron X-ray Radiation Facility with Imaging Plate at High Pressure", Phys. Chem. Minerals, 26, 539-545, 1999.

59. Dubrovinsky, L.S., Saxena, S.K., Lazor, P., "Stability of ß-iron: A New Synchrotron x-ray Study of Heated Iron at High Pressure", Eur. J. Mineral., 10, 43-47, 1998.

60. Hung, P.K., Nhan, N.T. and Vinh, L.T., "Molecular Dynamic Simulation of Liquid Al_2O_3 under Densification", Modelling and Simulation in Materials Science and Engineering, Issue Vol. 17, Issue 2, 025003, pp. 1-10, 2009.

61. Cazorla, C., Alfe, D. and Gillan, M.J., "Comment on "Molybdenum at High Pressure and Temperature: Melting From Another Solid Phase", Physical Review Letters, Vol 101, 049601, p. 1, 2008.

62. Belonoshko, A.B., Burakovsky, L., Chen, S.P., Johansson, B., Mikhaylushkin, A.S., Preston, D.L., Simak, S.I. and Swift, D.C., "Molybdenum at High Pressure and Temperature: Melting from Another Solid Phase", Physical Review Letters, Vol. 100, No. 13 135701, pp. 1-4, 2008.

63. Funamori, N. and Jeanloz, R., "High-Pressure Transformation of Al_2O_3" .Science, Vol 278, no 5340, pp. 109-1111, 1997.

64. Miller, G.H., Thomas, J.A. and Edwards, M.S., "The Equation of State of Molybdenum at 1400 ^{o}C", Journal of Applied Physics, Vol. 63, No. 9, pp. 4469-4475, 1988.

DOCUMENT CONTROL DATA

(Security classification of title, body of abstract and indexing annotation must be entered when the overall document is classified)

1. ORIGINATOR (the name and address of the organization preparing the document. Organizations for who the document was prepared, e.g. Establishment sponsoring a contractor's report, or tasking agency, are entered in Section 8.)

   TimeScales Scientific Ltd.
   554 Aberdeen Street SE
   Medicine Hat, AB T1A 0R7

2. SECURITY CLASSIFICATION
   (overall security classification of the document, including special warning terms if applicable)

   Unclassified

3. TITLE (the complete document title as indicated on the title page. Its classification should be indicated by the appropriate abbreviation (S, C or U) in parentheses after the title).

   A Review of Equation of State Models, Chemical Equilibrium Calculations and CERV Code Requirements for SHS Detonation Modelling

4. AUTHORS (Last name, first name, middle initial. If military, show rank, e.g. Doe, Maj. John E.)

   Thibault, Paul

5. DATE OF PUBLICATION (month and year of publication of document)

   October 2009

6a. NO. OF PAGES (total containing information, include Annexes, Appendices, etc) 50

6b. NO. OF REFS (total cited in document) 64

7. DESCRIPTIVE NOTES (the category of the document, e.g. technical report, technical note or memorandum. If appropriate, enter the type of report, e.g. interim, progress, summary, annual or final. Give the inclusive dates when a specific reporting period is covered.)

   Contract Report

8. SPONSORING ACTIVITY (the name of the department project office or laboratory sponsoring the research and development. Include the address.)

   Defence R&D Canada – Suffield, PO Box 4000, Station Main, Medicine Hat, AB T1A 8K6

9a. PROJECT OR GRANT NO. (If appropriate, the applicable research and development project or grant number under which the document was written. Please specify whether project or grant.)

   Gasless Detonation TIF (12qn05)

9b. CONTRACT NO. (If appropriate, the applicable number under which the document was written.)

   Subcontract for W7702-08R183/001/EDM

10a. ORIGINATOR'S DOCUMENT NUMBER (the official document number by which the document is identified by the originating activity. This number must be unique to this document.)

   DRDC Suffield CR 2010-013

10b. OTHER DOCUMENT NOs. (Any other numbers which may be assigned this document either by the originator or by the sponsor.)

11. DOCUMENT AVAILABILITY (any limitations on further dissemination of the document, other than those imposed by security classification)

   (x) Unlimited distribution
   ( ) Distribution limited to defence departments and defence contractors; further distribution only as approved
   ( ) Distribution limited to defence departments and Canadian defence contractors; further distribution only as approved
   ( ) Distribution limited to government departments and agencies; further distribution only as approved
   ( ) Distribution limited to defence departments; further distribution only as approved
   ( ) Other (please specify):

12. DOCUMENT ANNOUNCEMENT (any limitation to the bibliographic announcement of this document. This will normally corresponded to the Document Availability (11). However, where further distribution (beyond the audience specified in 11) is possible, a wider announcement audience may be selected).

   Unlimited

13. ABSTRACT (a brief and factual summary of the document. It may also appear elsewhere in the body of the document itself. It is highly desirable that the abstract of classified documents be unclassified. Each paragraph of the abstract shall begin with an indication of the security classification of the information in the paragraph (unless the document itself is unclassified) represented as (S), (C) or (U). It is not necessary to include here abstracts in both official languages unless the text is bilingual).

This report has summarized the current CERV capabilities and limitations and has identified possible models that could be added to the code for condensed and gaseous phase modelling. Particular attention has been given in the discussion to the implementation of suitable equations of state and melting models for condensed species along with databases for the model parameters. In order to assist in identifying and characterizing the CERV strengths and deficiencies, comparisons have been made with other codes for the constant pressure combustion temperatures of selected mixtures. The codes used for comparisons include FactSage, CEA and Thermo. The various codes have been applied to the Ti-Si and Ti-B systems and to the thermite systems, MoO_3-Al and Fe_2O_3-Al. Based on the models reviewed and the calculations performed, the CERV limitations have been summarized in terms of their level of importance to SHS modelling and the impact they may have on various sections of the CERV code.

14. KEYWORDS, DESCRIPTORS or IDENTIFIERS (technically meaningful terms or short phrases that characterize a document and could be helpful in cataloguing the document. They should be selected so that no security classification is required. Identifies, such as equipment model designation, trade name, military project code name, geographic location may also be included. If possible keywords should be selected from a published thesaurus, e.g. Thesaurus of Engineering and Scientific Terms (TEST) and that thesaurus-identified. If it is not possible to select indexing terms which are Unclassified, the classification of each should be indicated as with the title.)

Equations of State
Condenses Species
Cold Compression
Thermal Pressure and Expansion
Melting of Metals
Ab Initio Calculations
Equilibrium Calculations for SHS Systems of Interest
Thermite Systems
CERV

Defence R&D Canada

Canada's Leader in Defence
and National Security
Science and Technology

R & D pour la défense Canada

Chef de file au Canada en matière
de science et de technologie pour
la défense et la sécurité nationale

www.drdc-rddc.gc.ca